ChemComm

Catalytic Nucleic Acids (DNAzymes) as Functional Units for Logic Gates and Computing Circuits: From Basic Principles to Practical Applications

Journal:	*ChemComm*
Manuscript ID:	CC-FEA-12-2014-009874.R1
Article Type:	Feature Article
Date Submitted by the Author:	30-Dec-2014
Complete List of Authors:	Orbach, Ron; The Hebrew University of Jerusalem, Institute of Chemistry; Willner, Bilha; The Hebrew University of Jerusalem, Institute of Chemistry Willner, Itamar; The Hebrew University of Jerusalem, Institute of Chemistry

Catalytic Nucleic Acids (DNAzymes) as Functional Units for Logic Gates and Computing Circuits: From Basic Principles to Practical Applications

*Ron Orbach, Bilha Willner and Itamar Willner**

Institute of Chemistry, The Hebrew University of Jerusalem, Jerusalem 91904, Israel

*E-mail: willnea@vms.huji.ac.il Tel: 972-2-6585272. Fax: 972-2-6527715

Introduction

The base sequence in DNA encodes substantial structural and functional information into the biopolymer. Besides the Watson-Crick base-pairing of complementary nucleotide bases by hydrogen bonds, the self-assembly of guanosine bases into G-quadruplex,[1] the pH-stimulated formation of i-motif [2] or triplex DNA[3] nanostructures, and the cooperative formation of metal-ion-bridged duplex structures composed of C-Ag^+-C or T-Hg^{2+}-T,[4] are well established structural motifs of DNA. Functional features of DNA include sequence-specific recognition properties of nucleic acids (aptamers) toward low-molecular-weight substrates, macromolecules, biopolymers and even cells.[5] Similarly, sequence-specific nucleic acids may possess catalytic functions (DNAzymes), such as cleavage, ligation or phosphorylation.[6] The formation of DNA nanostructures, their dynamic transitions, separation, and reconfiguration of DNA assemblies are dictated by the energetics associated with different structural motifs of the oligonucleotides, Figure 1. For example, the stability of DNA duplexes is controlled by the number of base-pairs and their nature,[7] by the stabilization of the duplexes by metal-ion bridges, and by environmental factors, such as pH, ionic-strength, and temperature. Also, the ion-induced stabilization of G-quadruplexes (e.g. by K^+ or NH_4^+-ions), the hydrogen bonded i-motif structures or the formation of aptamer-substrate complexes may compete with the formation of DNA duplexes. These unique properties of DNA provide an arsenal of tools to use DNA as a functional material for DNA nanotechnology,[8] a rapidly developing high-impact area.

Different inter-linked research areas comprise the field of DNA nanotechnology, and these include the development of DNA-based sensors,[9] the assembly of one-, two- and three-dimensional DNA nanostructures[10] and their use as templates for the controlled spatial organization of biomolecules or nanoparticles,[11] the fabrication of DNA machines in solutions[12] or on surfaces,[13] and the design of stimuli-responsive DNA based hydrogels.[14]

The stimulus-driven reconfiguration of DNA nanostructures, and the control of their functions, may be considered as a macromolecular apparatus that mimics Boolean logic gate operations. In fact, substantial recent research efforts were directed to the implementation of molecular units to assemble Boolean logic gate operations.[15] Different molecule-based logic systems, such as unimolecular half-adder,[16] half-substractor,[17] full-adder,[18] multiplexer[19] and demultiplexer[20] systems were reported. The use of DNA as functional material for logic gates and computing circuits reveals, however, several advantages as the base sequence encoded in the DNA provides a rich arsenal to design functional components for logic and computing applications. The nucleic acid sequences that trigger the formation or reconfiguration of DNA structures might be considered as inputs, while the separation of nucleic acid units or their reorganization into new structures may provide output signals for the gate operation. Furthermore, the recognition properties of DNA (aptamers) and the formation of aptamer-ligand complexes, the cooperative formation of duplex DNA, in the presence of ions, or the pH-induced formation of i-motif or triplex nanostructures provide the use of additional inputs such as molecular/macromolar ligand, pH or metal ions.[21] Also, the catalytic functions of nucleic acids (DNAzymes) formed in upon the computational operation may lead to the amplification of the output signals. Indeed, DNA has been extensively implemented to develop DNA computing systems.[22] Different DNA nanostructures were used to perform logic gate operations,[23] and ingenious computing circuits and devices were demonstrated using the strand-displacement mechanism[24] or the programmed cleavage of DNA templates by enzymes.[25] The present feature article addresses the use of DNAzymes as functional units for the assembly of logic-gates and computing circuits (e.g. logic-gate cascades). Particularly, we aim to discuss the analogy between logic arrays and biological systems, and to present potential future application of these systems for sensing, nanomedicine, and as functional "smart" drug-delivery materials.

1. *Metal-Dependent DNAzymes as Computational Modules*

Metal-dependent DNAzymes, and particularly hydrolytic DNAzymes, are characterized by conserved sequences that accommodate the respective metal-ions, and variable "arms" that hybridize with the appropriate substrates (often a ribonucleobase-containing substrate).[26] The substrates are cleaved by the DNAzyme and the fragmented products are separated from it, thus allowing the regeneration of the catalytic functions of the DNAzyme. The DNAzymes exhibit different pH-dependence features, while some of the DNAzymes reveal optimal activities at neutral pH values, and lack activities in acidic media, other DNAzymes exhibit high activities at acidic conditions and are inactive in neutral media. Chemical manipulation of the DNAzyme sequences allows molecular engineering and the construction of structures exhibiting new functions and properties, as exemplified with the Mg^{2+}-dependent DNAzyme in Figure 2(A): (a) the loop region of the DNAzyme may be cleaved into two inactive subunits, (**1**) and (**2**), that may be modified by pre-designed domains, I and II. An auxiliary strand (**3**), that includes complementary sequences I' and II' may then bridge the subunits and assemble the active DNAzyme structure. (b) The substrates may be functionalized with different fluorophore/quencher (F/Q) units. While the fluorophores are quenched in the intact structure of the substrates, the cleavage of the substrates leads to the fluorescence of the optical label, associated with the fragmented products. The flexibility to structurally engineer the metal-dependent DNAzymes, and their substrates, enabled the development of a generic approach to construct a modular DNAzyme-based computing paradigm that is outlined in Figure 2(B).[27] The system consists of a library of DNAzyme subunits and a library of DNAzyme substrates. In the presence of the appropriate input(s), the input-guided assembly of the computing module proceeds, where the respective subunits form the Mg^{2+}-dependent DNAzyme that binds the substrate, thus yielding the computing module. The resulting cleaved product and its fluorescence provide the output for the respective input(s).

Accordingly, by using this paradigm a universal set of logic gates was constructed. Figure 2(C) depicts the Mg^{2+}-dependent subunits (**4**) - (**10**), a collection of the substrates (**11**) - (**13**), and the input strands I_1 and I_2. The input-guided structures lead to the dictated fluorescence associated with the different substrates (F_1-F_3). Figure 2(D) depicts the fluorescence features generated by the different structures and the derived truth table. Evidently, the system yields half-adder (HA) and half-subtractor (HS) logic operations that function as parallel devices in a reaction ensemble.

This basic concept was further extended to assemble logic-circuits. Figure 3(A) exemplifies the use of the library of DNAzyme subunits to drive a YES-AND-InhibAND logic gate cascade. Thus, the substrate structure, X, was modified to include a single-stranded ribonucleobase-containing loop, I, and two duplex domains II/IV and III/V. The loop I provides the substrate sequence for the DNAzyme, and upon the DNAzyme-stimulated cleavage of the loop, the sequence III is released, due to insufficient base pair stability, and the single strand V is tethered to the fragmented substrate as overhang. The resulting fragmented strands III and V may then act as input(s) for downstream gates. Accordingly, a library of the Mg^{2+}-dependent DNAzyme subunits, composed of the strands (**14**) – (**19**), the structurally-modified substrates (**20**) and (**21**) and the fluorophore/quencher-functionalized substrate (**22**) were constructed. In the presence of the input strands I_1, I_2 and I_3 the YES-AND-InhibAND logic-circuit was driven. The cleavage of the substrate (**22**) by the terminal InhibAND gate provided a fluorescence signal that reported the performance of the chain of gates, Figure 3(B). The truth-table corresponding to the three-gate cascade is also depicted in Figure 3(B). By a similar approach a cascade of YES gates was demonstrated, Figure 3(C). [27]

The pH-dependence of metal ions-dependent DNAzymes was further implemented to develop pH-programmed logic-gates cascades.[28] The system is based on the Mg^{2+}-dependent DNAzyme, that reveals high activity at pH = 7.2, moderate activity at pH = 6.0 and lacks

activity at pH = 5.2, and on the UO_2^{2+}-dependent DNAzyme, that shows high activity at pH = 5.2, moderate activity at pH = 6.0 and no activity at pH = 7.2. Thus, by designing mixtures of the two DNAzyme subunits, logic cascades operating in three different reconfigurable programs at pH = 7.2, 6.0 or 5.2 were constructed, Figure 4(A). The library consists of the Mg^{2+} and UO_2^{2+}-dependent DNAzyme subunits the inputs, I_1, I_2 and I_3, and the substrates. At the different pH values, the respective DNAzyme structures are formed. Thus, at pH = 5.2, only the logic circuit I is triggered-on by the UO_2^{2+}-dependent DNAzyme, leading to the fluorescence of F_2 as output signal. At pH = 6.0 the logic circuit II is triggered-on and the Mg^{2+} and UO_2^{2+} DNAzymes act in parallel, leading to the fluorescence of F_1 and F_2 as output readout signals of the cascade. At pH = 7.2, the logic circuit III is activated by the Mg^{2+}-dependent DNAzyme subunits, leading to the fluorescence of the fluorophore F_1. Figure 4(B) depicts the fluorescence changes of the system upon subjecting the library of DNAzyme subunits/substrates to the three inputs I_1, I_2, I_3 and the derived truth-table. Evidently, the composite computing module enabled the pH-programmed powering of three computing circuits consisting of different logic gates cascades. Furthermore, the introduction of anti-input strands into the system allowed the resetting of the computing module by separating the input-guided gate assemblies through the formation of energetically-stabilized input/anti-input duplexes. The re-addition of inputs into the system enables, then, the re-activation of any of the three pH-dictated programs.

Regulatory cellular networks often involve scaffold proteins that in the presence of appropriate signals trigger different intracellular pathways, and even orthogonal transformations. Mimicking such biological systems, where the information is compressed in a single entity and then can be fanned-out, may be achieved by multiplexer/demultiplexer systems. A multiplexer is a circuit that includes n selectors and 2^n inputs and it selects and directs any of the inputs into a single output. The demultiplexer performs the reverse function

and it transforms a single input, in the presence of n selector units, into 2^n outputs. The Mg^{2+}-dependent DNAzyme computing module was implemented to construct 2:1 and 4:1 multiplexer systems.[29] This is exemplified in Figure 5(A) with the assembly of the 2:1 multiplexer system. The system consists of a library of the Mg^{2+}-dependent subunits (**32**) – (**35**) and the substrate (**36**) that is modified with fluorophore/quencher units. The computing module is subjected to inputs I_1 and I_2 and a selector unit S_1. In the presence of I_1, the input-guided assembly of subunits (**32**)/(**33**) proceeds, giving rise to the cleavage of the substrate and the release of the fluorophore-modified fragment that provides the output fluorescence signal. In the presence of the two inputs, I_1 and I_2 and the selector unit S_1, the inter-hybridization features between the selector, S_1, and the inputs lead to the guided selection of the DNAzyme subunits (**34**) and (**35**). The base-pair complementarities between the selector domain X and I_1 neutralize I_1, while the domain Y of the selector and Y' of I_2 yields a stable duplex that selects the subunits (**34**) and (**35**) to form the active DNAzyme structure. This results in the Mg^{2+}-dependent catalytic cleavage of the substrate (**36**). That is, the interaction of the computing module with the inputs and selector unit leads to a single fluorescence output. The logic scheme of the resulting 2:1 multiplexer, the truth-table and the experimental results of the 2:1 multiplexer are provided in Figure 5(B). Using similar concepts, the design of a 4:1 multiplexer system was demonstrated by the implementation of a more complex library of DNAzyme subunits, four inputs and two selector units. [29]

The assembly of the 1:2 demultiplexer system is schematically presented in Figure 6(A). The system includes three DNAzyme subunits, (**37**)-(**39**) and two substrate units, (**40**) and (**41**), modified each with different fluorophore/quencher pairs (F_1/Q_1 and F_2/Q_2). The system was subjected to a single input, I_1, in the presence or absence of the selector, S. In the absence of the selector, the input-guided assembly of the subunits (**37**) and (**38**) led to the formation of the Mg^{2+}-dependent DNAzyme that binds the substrate (**40**). The biocatalytic

cleavage of the substrate led to the fluorescence of the F_1-fragmented product as output. In turn, subjecting the computing module to input I_1, in the presence of the selector, led to the cooperative stabilization of the (**38**) and (**39**) DNAzyme subunits, due to cooperative binding of the inter-hybridized I_1-selector components to the DNAzyme subunits. The association of the substrate (**41**) to the resulting nanostructure led to the cleavage of the substrate, thus yielding the fluorescence of the F_2-fragmented product as second output signal. That is, a single input drove in the absence or presence of the selector to two different fluorescent outputs. The resulting fluorescence results could be formulated in the form of the truth-table and logic circuit outlined in Figure 6(B), and these are consistent with the operation of a 1:2 demultiplexer logic circuit.[29]

Mg^{2+}-dependent DNAzyme has been implemented to assemble a library of catalytic constructs that lead in the presence of appropriate inputs to a full-adder.[30] The library is composed of seven computational modules, Figure 7. Four of the computational modules, that yield the sum output, consist of the Mg^{2+}-dependent DNAzyme loop blocked by three hairpin domains. While the other three computational modules, that yield the carry output, include only two hairpin structures that block the arms of the Mg^{2+}-dependent DNAzyme, Figure 7(A). The principles to construct the computational module that is blocked by three hairpins are shown in Figure 7(B). The system is composed of the Mg^{2+}-dependent DNAzyme loop L_1 and its two substrate-binding "arms" X_i and X_j. The DNAzyme loop is rigidified by a duplex bridge Z/Z'. The "arms" X_i and X_j are extended by hairpin structures L_2 and L_3, where the stem region of L_2 and L_3 are complementary to the "arm" domains of the DNAzyme. In the computational modules that yield the sum output two hairpins exist in the closed structures, whereas one hairpin is opened by an appropriate unit, C_j. The inputs may interact with the closed hairpin structures (L_2, L_3 or L_4) or with the C_j-opened hairpin. For example, Figure 7(C) exemplifies the interactions of one of the seven structures with

inputs I_1-I_3, which lead to the opening of hairpins L_1 and L_2, and to the closure of L_4, thus releasing the arms of the DNAzyme toward the binding of the appropriate fluorophore/quencher-modified substrate and the activation of the DNAzyme. The cleavage of the substrate leads to the fluorescence of the fluorophore-modified fragmented product and this provides the output signal. Accordingly, the introduction of each of the inputs I_1, I_2 or I_3 or the combination of all inputs leads to their interaction with one of the four computational modules that yields the sum output. Whereas, the other three computational modules are activated only in the presence of a combination of two inputs: $I_1 + I_2$, $I_2 + I_3$ or $I_1 + I_3$ leading to the carry output signal.

The versatility of the paradigm that involves computational modules comprising DNAzyme subunits and their substrates was also implemented to develop a full-adder system.[31] The schematic composition of the hairpin-input structure is presented in Figure 8(A). The stem sequences b/b' retain the hairpin in the closed configuration and the extended 5' and 3' tethers include the encoded sequences for controlling the selection of the DNAzyme subunits from the library. In the specific example, the domains include the c', f and a, e domains, and these result in the selection of the subunits L_1 and L_2 from the library to yield the computing DNAzyme module. The association of the substrate S_1 leads to the Mg^{2+}-dependent DNAzyme-stimulated cleavage of S_1 and to the fragmented fluorescent F_1-product provides on output signal. Figure 8(B) depicts the computational modules of the full-adder and their interactions with the inputs, I_1, I_2 or I_3. The library of the full-adder system consisted of 14 sequence-engineered subunits (**42**)-(**55**) and two substrates, S_1 and S_2, functionalized with two different fluorophore/quencher pairs (F_1/Q_1 and F_2/Q_2). The three inputs exhibit a hairpin structure and its 5' and 3' ends are extended by single-stranded tethers that select the appropriate Mg^{2+}-dependent DNAzyme subunits from the library to generate the respective computing module, which cleaves the substrate to yield the output

signal. Subjecting the library to each of the inputs, I_1, I_2 or I_3 resulted in the computing modules P_1, P_2 or P_3. Interaction of the library with two inputs, $I_1 + I_2$, $I_1 + I_3$ or $I_2 + I_3$ yielded the structures P_4, P_5 and P_6. That is, the pre-encoding of the appropriate sequence domains in I_1, I_2 and I_3 resulted in energetically-stabilized inter-hybridized dimers of the inputs that selected DNAzyme subunits that yield additional computing modules. The association of the substrate S_2 to these units resulted in its cleavage and the formation of the F_2-modified fragmented product as carry output. Interaction of the library with a combination of all three inputs results in the cross-interaction of the structures P_4, P_5 and P_6 to form self-assembled polymer Mg^{2+}-dependent DNAzyme wire, P_7. The catalytic cleavage of the respective DNAzyme substrates S_1 and S_2 leads to the two fluorescent F_1- and F_2-modified products as sum and carry outputs, respectively.

The systems that were described in this section have introduced the use of libraries of metal-ion-dependent DNAzyme subunits and their substrates as constitutes for versatile computations. The input-guided selection of the DNAzyme subunits from the library, dictated the formation of appropriate computing modules and the operation of the respective logic gates and computing circuits. Several important features were revealed by this paradigm: (i) The availability of different metal-dependent DNAzymes allows the construction of composite DNAzyme subunits libraries, thus, enabling to enhance the complexity of the computing circuits. (ii) The method enabled the design of a universal set of logic gates and the construction of multi-input systems operating in parallel (full adder, multiplexer/demultiplexer). (iii) By the appropriate design of the substrates of the DNAzyme subunits cascaded computational modules were demonstrated, thus leading to logic circuits. (iv) pH-field programmable logic arrays consisting of modular pH-sensitive DNAzyme libraries were demonstrated. (v) The release of nucleic acids strands as a result of the DNAzyme-mediated cleavage reaction does not only yield inputs for cascades, but the

products can be implemented to design amplification feedback paths, and eventually could provide functional therapeutic units (see section 3).

2. *DNAzyme-driven logic gate cascades*

DNAzyme-based logic gates that yield as an output a second DNAzyme allow the amplification of the final output signal. In this section we will present several methods to generate DNAzyme-logic gate cascades.

The UO_2^{2+}-dependent DNAzyme and the Mg^{2+}-dependent DNAzyme were implemented to construct an AND logic gate DNAzyme cascade,[32] Figure 9(A). The system consists of a DNA scaffold, (**56**), which includes two ribonucleobase-containing domains I and II that provide substrates for the UO_2^{2+}- and the Mg^{2+}-dependent DNAzymes, respectively. The two domains were inter-linked by the G-rich domain, X, which includes the base sequence to yield the G-quadruplex. In the presence of the appropriately designed UO_2^{2+}- and Mg^{2+}-dependent sequences, L_1 and L_2, their hybridization with the scaffold, (**56**) blocked the G-rich domain, and yielded the respective DNAzyme/substrate assemblies. While in the presence of either UO_2^{2+} or Mg^{2+} as input, only one of the substrates domains is cleaved off, retaining the G-rich domain in a blocked configuration. Subjecting the scaffold to the two inputs, UO_2^{2+}- and Mg^{2+} ions, (AND gate) leads to the cleavage of the two substrate domains I and II, resulting in the fragmented free G-quadruplex strand. The association of hemin to the resulting G-quadruplex yields, then, the hemin/G-quadruplex DNAzyme that catalyzes the oxidation of 2,2'-azinobis(3-ethylbenzothiazoline-6-sulfonic acid), $ABTS^{2-}$, by H_2O_2 to the colored product, $ABTS^{\bullet-}$, that provides an output signal for the DNAzyme cascade induced by the AND gate. Figure 9(B) depicts the readout of the AND gate operation through the cascade. By a related approach an OR gate operated by the UO_2^{2+} or Mg^{2+} inputs, coupled to the hemin/G-quadruplex output was constructed.[32]

The cooperative self-assembly of the Mg^{2+}-dependent DNAzyme subunits by allosteric components was used to activate an AND gate and to couple the hydrolytic function of the resulting DNAzyme to the horseradish peroxidase (HRP)-mimicking DNAzyme, providing the output signal for the bi-DNAzyme cascade.[33] This is exemplified in Figure 10 with the cocaine-stimulated allosteric activation of the Mg^{2+}-dependent DNAzyme that activates the secondary HRP-mimicking DNAzyme. The system consists of two subunits (**57**) and (**58**) that include three sub-domains. The domains I and I' correspond to the cocaine aptamer subunits, the domains II and II' include the subunits comprising the loop region of the Mg^{2+}-dependent DNAzyme, and the III and III' sequences that correspond to the domains complementary to the substrate of the Mg^{2+}-dependent DNAzyme. Also, the quasi-circular strand (**59**), which includes the ribonucleobase-functionalized sequence that acts as substrate for the Mg^{2+}-dependent DNAzyme is included in the system. Its domains IV and V include the G-rich sequences capable to self-assemble into the G-quadruplex. In the quasi-circular structure of (**59**) the formation of the G-quadruplex is prohibited due to partial blocking within the quasi-circular structure. All of the components of the system are separated due to insufficient inter-component hybridization stabilities. In the presence of cocaine and Mg^{2+} as inputs, the formation of the cocaine-aptamer subunits cooperatively stabilizes the hybridization of the Mg^{2+}-dependent DNAzyme subunits with the quasi-circular substrate. The binding of Mg^{2+}-ions to the DNAzyme sequence promotes the cleavage of the substrate, (**59**), and stimulates the release of the two G-quadruplex units. The association of hemin to the G-quadruplex nanostructures yields the hemin/G-quadruplex DNAzyme that catalyzes the oxidation of $ABTS^{2-}$ to the colored product $ABTS^{\bullet-}$. This provides an output signal for the AND gate induced bi-DNAzyme cascade.

A related system has implemented the selective cooperative stabilization of duplex nucleic acid by cytosine-Ag^{+}-cytosine inter-strand complexes, which enabled the activation

of the Mg^{2+}-dependent DNAzyme/hemin/G-quadruplex DNAzyme cascade,[34] Figure 11. The nucleic acids (**60**) and (**61**) include the domains I and II that correspond to the Mg^{2+}-dependent DNAzyme, the domains III and IV are complementary to the substrate-sequence of the DNAzyme, and the domains V and VI that reveal base complementarities and a C-C base mismatch. Also, a hairpin structure (**62**) that includes in its loop domain the ribonucleobase sequence that comprises the substrate for the Mg^{2+}-dependent DNAzyme is included in the system. The stem region of the hairpin structure includes the G-quadruplex sequence in a blocked configuration, domain VII. The subunits (**60**) and (**61**) and the substrate (**62**) do not exhibit sufficient base-pair stabilization to form a stable inter-strand nanostructure. However, in the presence of Ag^{+}-ions, as one input, the formation of the C-Ag^{+}-C bridges between domains V and VI, results in a stable duplex structure between (**60**) and (**61**). This duplex cooperatively stabilizes the hybridization of the domains III and IV to the substrate (**62**) while generating the active loop structure of the subunits I and II that comprise the Mg^{2+}-dependent DNAzyme. In the presence of Mg^{2+}-ions, as second input, the AND logic gate-stimulated cleavage of the substrate (**62**) leads to the fragmentation of the G-rich sequence VII that self-assembles in the presence of hemin to the hemin/G-quadruplex DNAzyme, and this provides the output colorimetric signal through the formation of $ABTS^{\bullet-}$.

An interesting DNAzyme multilayer cascade was reported using a structured chimeric substrate, SCS, as a functional scaffold,[35] Figure 12(A). The SCS scaffold, (**63**), consisted of a hairpin structure I that is linked at its one end to an outer strand Z, and modified at its second end with a loop domain Y extended with a domain Z' complementary, in part, to the outer strand Z. Part of the domain Z' acts as a ribonucleobase-sequence acting as substrate for the Zn^{2+}-dependent DNAzyme. Subjecting the SCS substrate, (**63**), to the DNAzyme sequence, (**64**), in the presence of Zn^{2+}-ions leads to strand displacement of the outer strand Z, and to the reconfiguration of the SCS to the nanostructure M_1. The DNAzyme-mediated

cleavage of M_1 leads to a hairpin fragmented product, M_2, and to the release of the Zn^{2+}-dependent DNAzyme (**64**). The system included as an initially passive unit a different Zn^{2+}-DNAzyme sequence, M_4, which was blocked by an inhibitor strand M_3. The fragmented hairpin product, M_2, generated by the first catalytic DNAzyme cycle includes the encoded information to displace the second DNAzyme sequence, M_4, while forming the energetically stabilized M_2/M_3 duplex. The DNAzyme sequence M_4 includes, however, binding "arms" that cannot interact with SCS (**63**). The resulting DNAzyme, M_4, may interact with another SCS substrate to activate a new catalytic cycle. Thus, the formation of DNAzyme by each catalytic layer amplifies the previous layer of cleavage of the SCS substrate. By the implementation of several passive DNAzyme/duplex nanostructures, the five layers amplification of the first DNAzyme-mediated cleavage of SCS was demonstrated. The DNAzyme generated in the final layer of the cascade cleaves a fluorophore/quencher-modified substrate, (**65**), and the resulting fluorescence provides the output signal for the multilayer cascade. The DNAzyme cascade operating in the presence of the SCS functional module was implemented to construct an AND logic cascade, and this was applied as dengue virus serotype sensor, Figure 12(B). The system consisted of a protected duplex structure composed of the Zn^{2+}-dependent DNAzyme sequence, L_1, blocked by the unit L_1' that included complementary region to the DNAzyme, extended by two tethers "a" and "b" that provide recognition domains for the Dengue A and DEN-k (dengue virus serotype markers) sequences. The system also includes the SCS module and a passive duplex structure L_2/L_2' that included a second Zn^{2+}-dependent DNAzyme sequence blocked by a sequence tethered at its end with a functional single strands capable to interact with the fragmented product of the SCS unit, "c", and a further recognition site for the Dengue B gene, "d". In the presence of the Dengue A and Dengue 1 as inputs (AND-gate), the duplex L_1/L_1' is separated, leading to the release of the Zn^{2+}-dependent DNAzyme, L_1. The resulting DNAzyme interacts with

the SCS scaffold to yield the fragmented product that acts cooperatively as input together with the Dengue B sequence (second AND gate) to separate the duplex L_2/L_2'. The second DNAzyme, L_2, released from the duplex L_2/L_2' cleaves the fluorophore/quencher modified substrate, (**66**), and the resulting fluorescence provides the readout signal for the existence of the three genes.

Metal-dependent DNAzymes-coupled to the hemin/G-quadruplex HRP-mimicking DNAzyme were applied to develop a series of logic gates by implementing pre-engineered hybridization properties between the DNAzyme reaction products. For example, Figure 13(A) depicts the use of the Pb^{2+}- and the Cu^{2+}-dependent DNAzymes to construct an AND logic gate.[36] The system consists of the Pb^{2+}-dependent sequence (**67**), and its ribonucleobase-containing substrate, (**68**), as one functional unit, and the Cu^{2+}-dependent DNAzyme sequence (**69**) and its substrate (**70**) as a second functional unit. Each of the substrates (**68**) and (**70**) includes a G-quadruplex subunit that is "caged" in the DNAzyme/substrate complexes as a result of favored hybridization. Pb^{2+}-ions and Cu^{2+} act as the inputs for the system. In the presence of Pb^{2+} alone or Cu^{2+}-ions alone only one subunit of the G-quadruplexes is being released from the respective (**67**)/(**68**) or (**69**)/(**70**) supramolecular complexes, and thus the formation of the G-quadruplex is prohibited. In the presence of Pb^{2+} and Cu^{2+}-ions, the cleavage of both of the substrates proceeds, and the fragmented subunits self-assemble into the G-quadruplex supramolecular structure. The binding of hemin to the resulting G-quadruplex yields the hemin/G-quadruplex DNAzyme that catalyzes the H_2O_2 oxidation of 3,3′,5,5′-tetrazmethylbenzidine sulfate, TMB, to the colored product TMB^+ that provides a color output signal for the AND logic gate. Similarly, Figure 13(B) presents the assembly of the INHIBIT logic gate by the implementation of molecularly-engineered Pb^{2+} and Cu^{2+}-dependent DNAzymes. The Pb^{2+}-dependent DNAzyme sequence (**71**) and its substrate (**72**) comprise one functional unit of the gate. The

substrate (**72**) includes the G-quadruplex sequence that is "caged" in the supramolecular (**71**)/(**72**) structure. The second functional unit of the gate is composed of the Cu^{2+}-dependent DNAzyme (**73**) and its substrate (**74**). The substrate (**74**) that is hybridized with the Cu^{2+}-dependent DNAzyme is pre-tailored to include a complementary domain to the G-quadruplex sequence. Accordingly, in the presence of Pb^{2+}-ions the catalytic Pb^{2+}-dependent DNAzyme supramolecular structure is activated, giving rise to the cleavage of the substrate (**72**), and to the assembly of the fragmented substrate into the G-quadruplex structure. The subsequent binding of hemin to the resulting G-quadruplex yields the hemin/G-quadruplex DNAzyme that catalyzes the H_2O_2-mediated oxidation of TMB to the colored product, as output. In the presence of Cu^{2+}-ions the DNAzyme/substrate complex (**73**)/(**74**) is activated and the cleavage of (**74**) yield a fragmented product that is catalytically inactive in the presence of hemin. In the presence of Pb^{2+} and Cu^{2+}-ions as inputs, both of the DNAzyme modules are activated. The complementarity of the fragmented products generated by the two DNAzyme leads to an energetically favored duplex that knocks out the fragmented product generated by the Pb^{2+}-dependent DNAzyme, thus, prohibiting the formation of the hemin/G-quadruplex DNAzyme, and to a "0" output. That is, output signals of the system generated by the enzyme cascade, Figure 13(C), follows an INHIBIT logic gate operation.

The different DNAzyme logic gate cascades discussed in this section have implemented metal-dependent cleavage DNAzymes and the hemin/G-quadruplex DNAzyme as catalytic ingredients for the logic gate cascades. The metal dependent Cu^{2+}-dependent ligation DNAzyme and the hemin/G-quadruplex were, similarly, applied to design logic gate cascades.[37] This is exemplified in Figure 14(A) with the assembly of an AND logic gate that used Hg^{2+} and Cu^{2+}-ions as inputs, and the Cu^{2+}-dependent DNAzyme as computing module that is conjugated to the hemin/G-quadruplex to yield the DNAzyme cascade. The nucleic acid (**75**) is folded in the presence of Hg^{2+}-ions into active Cu^{2+}-dependent DNAzyme and the

strand (**76**) is functionalized at its 3'-end with the imidazol-phosphate active group. The strands (**75**) and (**76**) are extended at their 3'-end and 5'-end, respectively, with subunits that can, under appropriate conditions self assemble into a G-quadruplex. At high ionic strength, the hybridization between (**75**) and (**76**) is energetically stable, and this allows, in the presence of Cu^{2+}-ions, the ligation of the components to yield ligated product (**77**). Upon turning the ionic strength of the system to a low salt concentration, the non-ligated duplex (**75**)/(**76**) separates into the individual strands. In turn, the ligated product stabilizes under these conditions the cooperative formation of the stable G-quadruplex. The binding of hemin to the G-quadruplex yields the hemin/G-quadruplex DNAzyme that catalyzes the H_2O_2-stimulated oxidation of $ABTS^{2-}$ to $ABTS^{\bullet-}$ or catalyzes the generation of chemiluminescence by the H_2O_2-induced oxidation of luminol. The system functions as an AND gate (Hg^{2+} and Cu^{2+}-ions act as inputs) that is coupled to hemin/G-quadruplex DNAzyme that provides the output signal for the bi-DNAzyme cascade. Besides the value of the system as a logic gate-driven DNAzyme cascade, the system provides an amplified sensing platform for Hg^{2+}-ions. Since the Cu^{2+}-induced ligation process is controlled by the concentration of Hg^{2+}-ions, the content of the ligated product, and the resulting hemin/G-quadruplex activity, are dictated by the concentration of Hg^{2+}. Figure 14(B) shows the chemiluminescence intensities generated by the bi-DNAzyme cascade in the presence of different concentrations of Hg^{2+} and the resulting calibration curve. The system enabled the highly selective analysis of Hg^{2+}-ions with detection limit corresponding to 10 nM. A related system has implemented cocaine and Cu^{2+}-ions as inputs, and the Cu^{2+}-dependent ligation DNAzyme as functional unit for the activation of an AND-gate-driven bi-DNAzyme cascade,[37] Figure 14(C). The system consisted of the imidazol-phosphate-modified nucleic acid, (**76**), and the nucleic acid (**78**), which included the Cu^{2+}-dependent ligation DNAzyme sequence and the cocaine aptamer sequence. The nucleic acid (**78**) was blocked by the strand (**79**). The strands (**76**) and (**78**)

were extended with the G-quadruplex subunits. At high ionic strength, and in the presence of cocaine, the blocker unit, (**79**), is displaced while forming the cocaine aptamer complex. Under these conditions the Cu^{2+}-dependent DNAzyme is configured, resulting in the ligation of the units (**76**) and (**78**) to yield the ligated product (**80**). The resulting product cooperatively stabilizes even at low salt concentrations, the G-quadruplex nanostructure. The association of hemin to the G-quadruplex conjugated ligated product leads to the hemin/G-quadruplex DNAzyme, that catalyzes the H_2O_2-mediated oxidation of $ABTS^{2-}$ to $ABTS^{\bullet-}$ or generates chemiluminescence through the catalyzed oxidation of luminol by H_2O_2. Thus, cocaine and Cu^{2+} act as the inputs for and AND gate driven bi-DNAzyme cascade, where the colored $ABTS^{\bullet-}$ or the chemiluminescence generated by the hemin/G-quadruplex provide the output for the DNAzyme cascade and the AND gate operation. As the content of the conjugated structure consisting of the ligation DNAzyme and the hemin/G-quadruplex HRP-mimicking DNAzyme is controlled by the concentration of the cocaine, the output signal relates to the concentration of cocaine. Indeed, the system was implemented to analyze cocaine. Figure 14(D) depicts the chemiluminescence intensities generated by the system in the presence of different concentrations of cocaine, and the resulting calibration curve. The system enables the analysis of cocaine with a detection limit that corresponded to 2.5 μM.

3. *Applications of DNAzyme-base logic gates*

The activation of DNA-based logic gates by diverse inputs, such as nucleic acid strands, aptamer-substrates and metal ions, and the different optical outputs of the systems, paved the way to implement the systems for different sensing applications, multiplexed sensing of analytes, and amplified sensing. These applications of DNAzyme based logic gates were briefly addressed in the previous sections. Recent studies demonstrated, however, other applications of DNAzyme-driven logic systems that highlighted diverse potential uses

of these systems in other different disciplines. For example, DNAzyme-modified mesoporous SiO_2 nanoparticles (NPs) have been applied as functional units for the multiplexed controlled release of two fluorescent dyes following an AND gate operation principles.[38] Figure 15(A) shows the structure of mesoporous SiO_2 NPs, MP-SiO_2-NPs, modified with the ribonucleobase (**81**) or (**82**) that act as substrates for the Mg^{2+}-dependent DNAzyme (NPs-A) or the Zn^{2+}-dependent DNAzyme (NPs-B), respectively. The NPs-A were loaded with the fluorescent dye methylene blue, MB^+ and the pores were capped with the Mg^{2+}-dependent DNAzyme sequence (**83**) resulting in the trapping of the dye in the pores. Similarly, the NPs-B were loaded with the fluorescence dye thionin, (Th) and the pores were capped with the Zn^{2+}-dependent DNAzyme sequence (**84**). Each of the MP SiO_2-NPs was selectively opened in the presence of Mg^{2+} or Zn^{2+}-ions as inputs, resulting in the release of MB^+ or Th from the respective porous NPs, Figure 15(B) and (C). By mixing the two different NPs the operation of an AND gate was demonstrated, Figure 15(D), panel I to IV. While in the presence of Mg^{2+} or Zn^{2+} the fluorescence of MB^+ or Th is observed (panels II and IV, respectively), subjecting the system to the two inputs resulted in the fluorescence of the two probes, panel IV, and the two fluorescence bands provide the output for the AND gate. A further system for the unlocking of the pores of mesoporous SiNPs and the release of the pore-entrapped substrate, using an AND logic gate operation, has implemented Mg^{2+}-ions and adenosine triphosphate, ATP, as inputs, Figure 16(A).[38] The system made use of the fact that incorporation of a random strand I into the loop sequence of the Mg^{2+}-dependent DNA turns the nucleic acid structure to be catalytically inactive, due to the flexibility of the enlarged loop. The rigidification of the extended loop, e.g., by the formation of an aptamer-substrate complex regenerated the catalytic function of the DNAzyme. Accordingly, the fluorescent probe MB^+ was loaded in the pores of the extended loop sequence of the Mg^{2+}-dependent DNAzyme (**85**). The locked SiO_2 NPs remained intact in the presence of Mg^{2+}-ions. In the

presence of ATP and Mg^{2+}-ions as inputs, the pores were unlocked and MB^+ was released, Figure 16(B) and (C). The AND gate logic operation of this system has important medical applications as a controlled drug release mechanism. Since ATP is overexpressed in cancer cells, the selective enhanced unloading of anti-cancer drugs in cancerous cells may be envisaged. Indeed, the (**85**)-modified SiO_2 NPs were loaded with the anti-cancer drug, doxorubicin (DOX). The effective release of the DOX from the pores being unlocked by the two inputs, e.g., ATP and Mg^{2+}-ions, was demonstrated (AND gate), Figure 16(D).

The concept of library of DNAzyme subunits and their substrates as logic gate computational modules, described in section 1 was implemented to probe diagnostically-significant miRNA and mRNA in intracellular environment.[39] The system is based on the construction of a library of DNAzyme subunits of the c-jun cleaving Dz13 DNAzyme. In the presence of the appropriate inputs, miRNA or mRNA, the input-guided assembly of the DNAzyme subunits occurred, with the cooperative binding of the fluorophore/quencher-functionalized substrate (**86**). This led to the cleavage of the substrate and to the generation of fluorescence as output signal. Specific inputs used in the study included miRNA31 (a breast specific miRNA), miR21 (a breast cancer miRNA), mir125b (health indicative miRNA) and c-myc oncogene (as cancer mRNA biomarker). Figure 17(A) exemplifies the use of the DNAzyme subunits library to operate the AND gate using miR21 and miR125b as the two inputs I_A and I_B. The DNAzyme subunit (**87**) (that includes a hairpin domain) and the subunit (**88**), are selected to form the active DNAzyme only in the presence of both inputs (I_A+I_B). Figure 17(B) depicts the fluorescence intensities generated by the system in the presence of the different inputs, indicating the operation of an AND gate. By a similar approach a variety of other logic gates, such as OR, NAND, ANDNOT (INHIBIT gate), XOR and NOR were demonstrated. Upon subjecting the DNAzyme library/substrate to the different inputs in a cell lysate the respective logic expression outlined in Figure 17(C), diagnosis combinations I or

II, were operated. The fluorescence changes observed in the different systems (reflected by the cleaved substrate), Figure 17(C), panel III, fit the expected diagnosis of the different miRNAs, mRNA (inputs) and the mixtures. The AND gate computational module was then applied to analyze the miRNA21 and miR125b injected into cancer cells. The micro-junction of the inputs and computational AND module led to the intracellular cleavage of the substrate. Figure 17(D) depicts the intracellular microscopic imaging of the selective cleavage of the substrate, only in the presence of the two inputs, panel I-IV, and the display of the quantitative fluorescence intensities of the cleaved substrate, Figure 17(E).

Further application of metal-ion dependent DNAzymes to power chemical transformations by logic operations has involved the ion-selective dissolution of DNA hydrogels and the activation of multi-enzyme cascades, Figure 18.[40] Acrydite nucleic acid (**89**) was used to synthesize acrylamide-acrydite nucleic acid copolymer chains P_1 and P_2. The chains were crosslinked by the Zn^{2+} or Mg^{2+} DNAzyme sequences (**90**) and (**91**) in the presence of the respective DNAzyme substrates (**92**) or (**93**). The crosslinking led to the formation of hydrogels. The two enzymes glucose oxidase, GOx, and HRP were entrapped in the hydrogels. Treatment of two pieces of the hydrogels with Zn^{2+}-ions and Mg^{2+}-ions resulted in the cleavage of the respective DNAzyme substrates, (**92**) and (**93**), and to the dissociation of the hydrogels. The released enzymes communicated one with another and the bienzyme cascade was activated. GOx mediated the aerobic oxidation of glucose to gluconic acid and H_2O_2 and the resulting hydrogen peroxide acted as substrate for HRP that catalyzed the oxidation of $ABTS^{2-}$, to the colored product. The bienzyme cascade was activated only in the presence of Mg^{2+} and Zn^{2+}-ions, AND logic gate. The process proceeded only in the presence of these two ions that stimulated the activation of the hydrogel-bridging DNAzyme and the separation of the hydrogels.

A possible therapeutic application of the computational module generated by the Mg^{2+}-dependent DNAzyme and its substrate (see section 1) was demonstrated by implementing a logic system acting as an autonomous sense-and-treat apparatus. Hemorrhage or shock events are accompanied by the excessive formation of thrombin that might cause blood clots and brain damages. As the thrombin aptamer binds thrombin and inhibits its hydrolytic activity, the logic release of the aptamer was suggested as a triggered therapeutic system.[27] Accordingly, the Mg^{2+}-dependent DNAzyme subunits (**94**) and (**95**) and the substrate (**96**) provided the logic module. The substrate included in a caged inactive configuration of the thrombin sequence (**97**). In the presence of the nucleic acid I_1 acting as input, the guided assembly of the Mg^{2+}-dependent DNAzyme and the cleavage of the substrate (**96**) occurred, Figure 19(A). The cleavage of the substrate released the aptamer unit (**97**) and this reconfigured into the aptameric G-quadruplex/thrombin complex, resulting in the hydrolytic activity of thrombin, Figure 19(B). Although the practical therapeutic applicability of such system is still far away, the system provides a paradigm that deserves further research efforts. For example, the guided assembly of the DNAzyme subunits via biomarkers and appropriate aptamer-ligand complexes may be a versatile route to release inhibiting aptamers for different other enzymes.

Conclusions and Perspectives

The present article has summarized the implementation of DNAzymes for logic gates and logic-circuits operation. Substantial progress has been demonstrated and DNAzymes provide an important component in the area of DNA computing. A universal set of logic gates, a full adder, multiplexer/demultiplexer, cascaded logic circuits, field programmable logic gates and computing circuits were developed using DNAzymes as computing modules. Despite the advances in the field, challenging research targets are, however, still ahead of us,

particularly efforts to find practical applications of the logic gate and computing circuitry systems.

From a fundamental point of view logic gate cascades mimic intracellular biosynthetic pathways and catalytic networks. The input-guided control of directional DNAzyme cascades, the input-controlled fan-out of several outputs that drive catalytic paths, and the pH programmable dictated control of logic circuits mimic cellular functionalities, such as dictated directional transformations, networking of catalytic processes branching of biocatalytic reactions, and more. Some of these analogies have been mentioned in the article, but many challenges need to be resolved. These include, for example, the amplification of biocatalytic cascade, the development of feedback mechanisms and the parallel operation of circuits by many inputs.

The application of DNAzyme-based logic circuits is still challenging. The assembly of computational catalytic modules through the recognition of an input and the subsequent physical readout signal represents the basic function of an amplified sensing. Particularly, the parallel input-guided assembly of several computational modules provides the basis for multiplexed sensing. Indeed, this interplay between logic gates and sensing phenomena was emphasized throughout the article. More sophisticated applications may be, however, envisaged. The controlled release of molecular or macromolecular components from “smart” carrier matrices, such as mesoporous nanoparticles or hydrogels, using logic gate operations, could provide new drug delivery and controlled release systems. Particularly, micro or nano particulate carriers that include “smart” locking/unlocking mechanisms could provide new therapeutic materials by implementing logic gate principles. For example, unlocking of such systems by biomarkers in cancer cells could provide mechanism for the release of blends of chemotherapeutic drugs. The dictated release of chemical components from carrier matrices, also, finds interesting applications in controlled and selective synthesis. Also, DNAzyme-

driven cascades could activate secondary catalytic reactions for the synthesis of catalytic scaffolds for the synthesis of new nanomaterials. For example, the outputs of the computing modules may activate secondary polymerization cycles such as the hybridization chain reactions (HCR) to yield DNAzyme wires (e.g., composed of hemin/G-quadruplexes) acting as catalytic templates for the synthesis of functional polymers, e.g., conducting polymers.

The incorporation of nucleic acid machineries, and particularly DNAzyme-based logic gate and computing circuits, into cells has implications for cell engineering and nanomedicine. These research activities are in their infancy, but several studies have demonstrated the viability of such concepts. For example, 2D and 3D RNA structures were integrated into the cellular transcription mechanism of cells, and cells of new functionalities and properties, such as programmed hydrogen-generating cells, were generated.[41] The preliminary results demonstrating the "logic" release of aptamers that inhibit enzymes,[27] and the successful logic gate release of siRNA into the nucleous of cancer cell lysates via DNAzyme constructs[39] demonstrate the potential future impact of logic circuitries on future nanomedicine. Nonetheless, many different challenges such as the biocompatibility of the systems, targeting of the nanostructures to cells, and the stabilization of the nanostructures against enzymatic digestion need to be resolved.

To conclude, the input-guided assembly of computational DNAzyme modules holds great promises for sensing, nanomedicine, material science and living technologies.

Acknowledgement: This research is supported by the FET Open EU program, MULTI project.

References

1. (a) M. Bansal, *Curr. Sci.,* 2003, **85**, 1556-1563; (b) J. L. Sessler, C. M. Lawrence, J. Jayawickramarajah, *Chem. Soc. Rev.,* 2007, **36**, 314-325; (c) J. T. Davis, G. P. Spada, *Chem. Soc. Rev.,* 2007, **36**, 296-313.

2. (a) D. Collin, K. Gehring, *J. Am. Chem. Soc*., 1998, **120**, 4069-4072; (b) J. L. Leroy, M. Gueron, J. L. Mergny, C. Helene, *Nucleic Acids Res*., 1994, **22**, 1600-1606; (c) S. Nonin, J. L. Leroy, *J. Mol. Biol.,* 1996, **261**, 399-414.

3. (a) A. Ldili, A. Vallée-Bélisle, F. Ricci, *J. Am. Chem. Soc*., 2014, **136**, 5836-5839; (b) V. Sklenar, J. Feigon, *Nature,* 1990, **345**, 836-838; (c) R. Haner, P. B. Dervan, *Biochemistry,* 1990, **29**, 9761-9765; (d) J. Volker, D. P. Botes, G. G. Lindsey, H. H. Klump, *J. Mol. Biol.,* 1993, **230**, 1278-1290.

4. (a) J. S. Lee, M. S. Han, C. A. Mirkin, *Angew. Chem., Int. Ed.,* 2007, **46**, 4093-4096; (b) Z. Zhu, Y. Su, J. Li, D. Li, J. Zhang, S. Song, Y. Zhao, G. Li, C. Fan, *Anal*. *Chem*., 2009, **81**, 7660-7666; (c) C. W. Liu, Y. T. Hsieh, C. C. Huang, H. T. Chang, *Chem. Commun.,* 2008, 2242-2244; (d) Y. Wen, F. Xing, S. He, S. Song, L. Wang, Y. Long, D. Li, C. Fan, *Chem. Commun.,* 2010, **46**, 2596-2598; (e) K. S. Park, C. Jung, H. G. Park, *Angew. Chem., Int. Ed.,* 2010, **49**, 9757-9760; (f) A. Ono, S. Q. Cao, H. Togashi, M. Tashiro, T. Fujimoto, T. Machinami, S. Oda, Y. Miyake, I. Okamoto, Y. Tanaka, *Chem. Commun.,* 2008, 4825-4827.

5. (a) C. Tuerk, L. Gold, *Science,* 1990, **249**, 505-510; (b) A. D. Ellington, J. W. Szostak, *Nature,* 1990, **346**, 818-822; (c) S. E. Osborn; A. D. Ellington, *Chem. Rev*., 1997, **97**, 349-370; (d) M. P. Robertson, A. D. Ellington, *Nat. Biotechnol*., 2001, **19**, 650-655.

6. (a) R. R. Breaker, G. F. Joyce, *Chem. Biol.,* 1994, **1**, 223-229; (b) I. Willner, B. Shlyahovsky, M. Zayats, B. Willner, *Chem. Soc. Rev.,* 2008, **37**, 1153-1165; (c) M.

Famulok, J. S. Hartig, G. Mayer, *Chem. Rev.,* 2007, **107**, 3715-3743; (d) G. F. Joyce, *Angew. Chem., Int. Ed.,* 2007, **46**, 6420-6436.

7. (a) D. Soloveichik, G. Seelig, E. Winfree, *Proc. Natl. Acad. Sci. U. S. A.,* 2010, **107**, 5393-5398; (b) D. Y. Zhang, A. J. Turberfield, B. Yurke, E. Winfree, *Science*, 2007, **318**, 1121-1125.
8. (a) C. H. Lu, B. Willner, I. Willner, *ACS Nano,* 2013, **7**, 8320-8332; (b) N.C. Seeman, *Trends Biochem. Sci.,* 2005, **30**, 119-125.
9. (a) I. Willner, M. Zayats, *Angew. Chem., Int. Ed.,* 2007, **46**, 6408-6418; (b) R. Freeman, J. Girsh, I. Willner, *ACS Appl. Mater. Interfaces,* 2013, **5**, 2815-2834; (c) D. M. Kolpashchikov, *Chem. Rev.*, 2010, **110**, 4709-4723; (d) Y. Du, B. Li, E. Wang, *Acc. Chem. Res.,* 2013, **46**, 203-213; (e) Y. V. Gerasimova, D. M. Kolpashchikov, *Chem. Biol.*, 2010, **17**, 104-106; (f) G. Pelossof, R. Tel-Vered, I. Willner, *Anal. Chem.*, 2012, **84**, 3703-3709; (g) C. H. Fan, K. W. Plaxco, A. J. Heeger, *Proc. Natl. Acad. Sci. U. S. A.,* 2003, **100**, 9134-9137; (h) Y. Du, B. Li, F. Wang, S. Dong, *Biosens. Bioelectron.,* 2009, **24**, 1979-1983; (i) Y. V. Gerasimova, E. M. Cornett, E. Edwards, X. Su, K. H. Rohde and D. M. Kolpashchikov, *ChemBioChem*, 2013, **14**, 2087-2090.
10. (a) C. Lin, Y. Liu, S. Rinker, H. Yan, *ChemPhysChem,* 2006, **7**, 1641-1647; (b) E. Winfree, F. Liu, L. A. Wenzler, N. C. Seeman, *Nature,* 1998, **394**, 539-544; (c) F. A. Aldaye, A. L. Palmer, H. F. Sleiman, *Science,* 2008, **321**, 1795-1799; (d) C. Mao, W. Sun, N. C. Seeman, *J. Am. Chem. Soc.,* 1999, **121**, 5437-5443; (e) J. Sharma, R. Chhabra, Y. Liu, Y. Ke, H. Yan, *Angew. Chem., Int. Ed.*, 2006, **45**, 730-735; (f) Y. Ke, L. Ong, W. Shih, P. Yin, *Science,* 2012, **338**, 1177-1183; (g) B. Ding, R. Sha, N. C. Seeman, *J. Am. Chem. Soc.,* 2004, **126**, 10230-10231; (h) Y. Weizmann, A. B. Braunschweig, O. I. Wilner, Z. Cheglakov, I. Willner, *Proc. Natl. Acad. Sci. U. S. A.,* 2008, **105**, 5289-5294; (i) P. W. K. Rothemund, *Nature,* 2006, **440**, 297-302; (j) S. Rinker, Y. Ke, Y. Liu, R.

Chhabra, H. Yan, *Nat. Nanotechnol*., 2008, **3**, 418-422; (k) E. S. Andersen, M. Dong, M. M. Nielsen, K. Jahn, R. Subramani, W. Mamdouh, M. M. Golas, B. Sander, H. Stark, C. L. P. Oliveira, J. S. Pedersen, V. Birkedal, F. Besenbacher, K. V. Gothelf, J. Kjems, *Nature,* 2009, **459**, 73-76; (l) Y. Ke, J. Sharma, M. Liu, K. Jahn, Y. Liu, H. Yan, *Nano Lett*., 2009, **9**, 2445-2447; (m) H. Ozhalici-Unal, B. A. Armitage, *ACS Nano,* 2009, **3**, 425-433.

11. (a) O. I. Wilner, I. Willner, *Chem. Rev.,* 2012, **112**, 2528-2556; (b) O. I. Wilner, Y. Weizmann, R. Gill, O. Lioubashevski, R. Freeman, I. Willner, *Nat. Nanotechnol*., 2009, **4**, 249-254; (c) C. M. Niemeyer, J. Koehler, C. Wuerdemann, *ChemBioChem,* 2002, **3**, 242-245; (d) F. Diezmann, O. Seitz, *Chem. Soc. Rev.,* 2011, **40**, 5789-5801; (e) S. Rinker, Y. Ke, Y. Liu, R. Chhabra, H. Yan, *Nat. Nanotechnol*., 2008, **3**, 418-422.
12. (a) R. P. Goodman, M. Heilemann, S. Doose, C. M. Erben, A. N. Kapanidis, A. J. Turberfield, *Nat. Nanotechnol*., 2008, **3**, 93-96; (b) C. Teller, I. Willner, *Curr. Opin. Biotechnol*., 2010, **21**, 376-391; (c) Y. Weizmann, Z. Cheglakov, B. Basnar and I. Willner, *Org. Biomol. Chem.,* **5**, 223-225; (d) F. Wang, B. Willner and I. Willner, *Top. Curr. Chem.,* 2014, **354**, 279-338.
13. (b) X. Liu, A. Niazov-Elkan, F. Wang, I. Willner, *Nano Lett.,* 2013, **13**, 219-225; (c) G. Pelossof, R. Tel-Vered, X. Liu, I. Willner, *Nanoscale,* 2013, **5**, 8977-8981.
14. (a) C. H. Lu, X. J. Qi, R. Orbach, H. H. Yang, I. Mironi-Harpaz, D. Seliktar and I. Willner, *Nano Lett.,* 2013, **13**, 1298-1302; (b) H. Lin, Y. Zou, Y. Huang, J. Chen, W. Y. Zhang, Z. Zhuang, G. Jenkins and C. J. Yang, *Chem. Commun.,* 2011, **47**, 9312-9314; (c) E. Cheng, Y. Xing, P. Chen, Y. Yang, Y. Sun, D. Zhou, L. Xu, Q. Fan and D. Liu, *Angew. Chem., Int. Ed.,* 2009, **48**, 7660-7663; (d) W. Guo, X. J. Qi, R. Orbach, C. H. Lu, L. Freage, I. Mironi-Harpaz, D. Seliktar, H. H. Yang, I. Willner, *Chem. Commun.,* 2014,

50, 4065–4068; (e) W. Guo, C. H. Lu, X. J. Qi, R. Orbach, M. Fadeev, H. Hao Yang, I. Willner, *Angew. Chem., Int. Ed.,* 2014, **53**, 10134-10138.

15. (a) A. P. de Silva , H. Q. N. Gunaratne , C. P. McCoy, *Nature,* 1993, **364**, 42–44; (b) A. Matteo, Z. Lei and A. Credi, *Coord. Chem. Rev.*, 2010, **254**, 2267–2280; (c) G. de Ruiter, M. E. van der Boom, *J. Mater. Chem.*, 2011, **21**, 17575-17581; (c) J. Andréasson, U. Pischel, *Chem. Soc. Rev.*, 2015, DOI: 10.1039/C4CS00342J.
16. X. Guo, D. Zhang, G. Zhang, D. Zhu, *J. Phys. Chem., B* 2004, **108**, 11942–11945.
17. S. J. Langford, T. Yann, *J. Am. Chem. Soc.,* 2003, **125**, 11198-11199.
18. D. Margulies, G. Melman, A. Shanzer, *J. Am. Chem. Soc.*, 2006, **128**, 4865-4871.
19. (a) J. Andréasson, S.D. Straight, S. Bandyopadhyay, R.H. Mitchell, T.A. Moore, A.L. Moore, D. Gust, *Angew. Chem. Int. Ed.,* 2007, **46**, 958-961; (b) M. Amelia, M. Baroncini, A. Credi, *Angew. Chem. Int. Ed.,* 2008, **47**, 6240-6243.
20. J. Andreasson, S. D. Straight, S. Bandyopadhyay, R. H. Mitchell, T. A. Moore, A. L. Moore and D. Gust, *J. Phys. Chem. C*, 2007, **111**, 14274–14278.
21. (a) S. Shimron, N. Magen, J. Elbaz, I. Willner, 2011, **47**, 8787-8789; (b) C. Teller, S. Shimron, I. Willner, 2009, **81**, 9114-9119; (c) J. Elbaz, S. Shimron, I. Willner, 2010, **46**, 1209-1211.
22. (a) M. N. Stojanovic, T. E. Mitchell, D. Stefanovic, *J. Am. Chem. Soc.,* 2002, **124**, 3555-3561; (b) M. N. Stojanovic, D. Stefanovic, *Nat. Biotechnol.*, 2003, **21**, 1069-1074; (c) L. Wang, J. Zhu, L. Han, L. Jin, C. Zhu, E. Wang, S. Dong, *ACS Nano,* 2012, **6**, 6659-6666. (d) R. Orbach, L. Mostinski, F. Wang, I. Willner, *Chemistry Eur. J.,* 2012, **18**, 14689-14694. (e) R. Orbach, F. Remacle, R. D. Levine, I. Willner, *Proc. Natl. Acad. Sci. U.S.A.,* 2012, **109**, 21228-21233.
23. (a) J. M. Picuri, B. M. Frezza, M. R. Ghadiri, *J. Am. Chem. Soc.,* 2009, **131**, 9368-9377; (b) N. C. Gianneschi, M. R. Ghadiri, *Angew. Chem., Int. Ed.,* 2007, **46**, 3955-3958.

24. (a) G. Seelig, D. Soloveichik, D. Y. Zhang, E. Winfree, *Science,* 2006, **314**, 1585-1588; (b) A. Padirac, T. Fujii, Y. Rondelez, *Curr. Opin. Biotechnol.,* 2013, **24**, 575-580; (c) L. Qian, E. Winfree, *Science,* 2011, **332**, 1196-1201; (d) L. Qian, E. Winfree, J. Bruck *Nature,* 2011, **475**, 368-372.

25. (a) Y. Benenson, T. Paz-Elizur, R. Adar, E. Keinan, Z. Livneh, E. Shapiro, *Nature,* 2001, **414**, 430-434; (b) Y. Benenson, B. Gil, U. Ben-Dor, R. Adar, E. Shapiro, *Nature,* 2004, **429**, 423-429; (c) R. Adar, Y. Benenson, G. Linshiz, A. Rosner, N. Tishby, E. Shapiro, *Proc. Natl. Acad. Sci. U. S. A.,* 2004, **101**, 9960-9965.

26. R. R. Breaker, *Nat. Biotechnol.*, 1997, **15**, 427-431.

27. J. Elbaz, O. Lioubashevski, F. Wang, F. Remacle, R. D. Levine, I. Willner, *Nat. Nanotechnol.,* 2010, **5**, 417-422.

28. J. Elbaz, F. Wang, F. Remacle, I. Willner, *Nano Lett.,* 2012, **12**, 6049-6054.

29. R. Orbach, F. Remacle, R. D. Levine, I. Willner, *Chem. Sci.*, 2014, **5**, 1074-1081.

30. H. Lederman, J. Macdonald, D. Stefanovic, M. N. Stojanovic, *Biochemistry*, 2006, **45**, 1194-1199.

31. R. Orbach, F. Wang, O. Lioubashevsky, R. D. Levine, F. Remacle, I. Willner, *Chem. Sci.*, 2014, **5**, 3381-3387.

32. M. Moshe, J. Elbaz and I. Willner, *Nano Lett.*, 2009, **9**, 1196-1200.

33. J. Elbaz, M. Moshe, B. Shlyahovsky and I. Willner, *Chem. Eur. J.*, 2009, **15**, 3411-3418.

34. S. Shimron, J. Elbaz, A. Henning, I. Willner, *Chem. Commun.*, 2010, **46**, 3250-3252.

35. C.W. Brown, M. R. Lakin, E. K. Horwitz, M. L. Fanning, H. E. West, D. Stefanovic, S. W. Graves, *Angew. Chem. Int. Ed.*, 2014, **53**, 7183-7187.

36. L. Zhang, Y. -M. Zhang, R. -P. Liang, J. -D. Qiu, *J. Phys. Chem. C,* 2013, **117**, 12352-12357.

37. F. Wang, R. Orbach, I. Willner, *Chem. Eur. J.*, 2012, **18**, 16030–16036.

38. Z. Zhang, D. Balogh, F. Wang, I. Willner, *J. Am. Chem. Soc.*, 2013, **135**, 1934-1940.

39. M. Kahan-Hanum, Y. Douek, R. Adar, E. Shapiro, *Sci. Rep.,* 2013, **3**, 1535.

40. S. Lilienthal, Z. Shpilt, F. Wang, I. Willner (*submitted for publication*).

41. C. J. Delebecque, A. B. Lindner, P. A. Silver, F. A. Aldaye, *Science* 2011, **333**, 470-474.

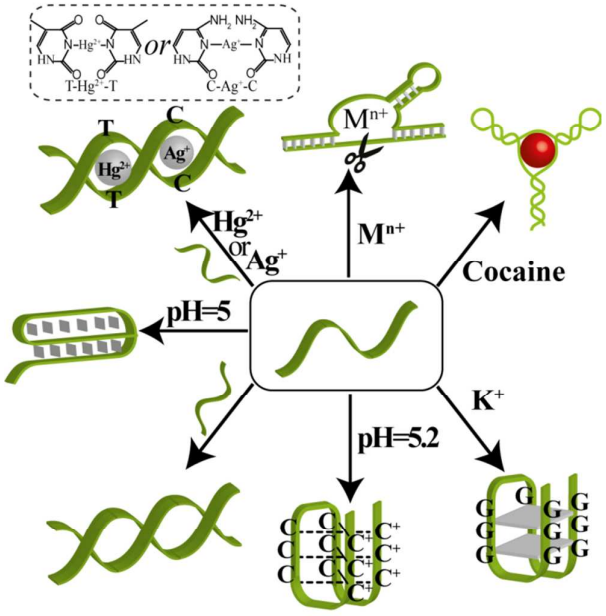

Figure 1: Structural and functional information encoded in the base sequence of nucleic acids.

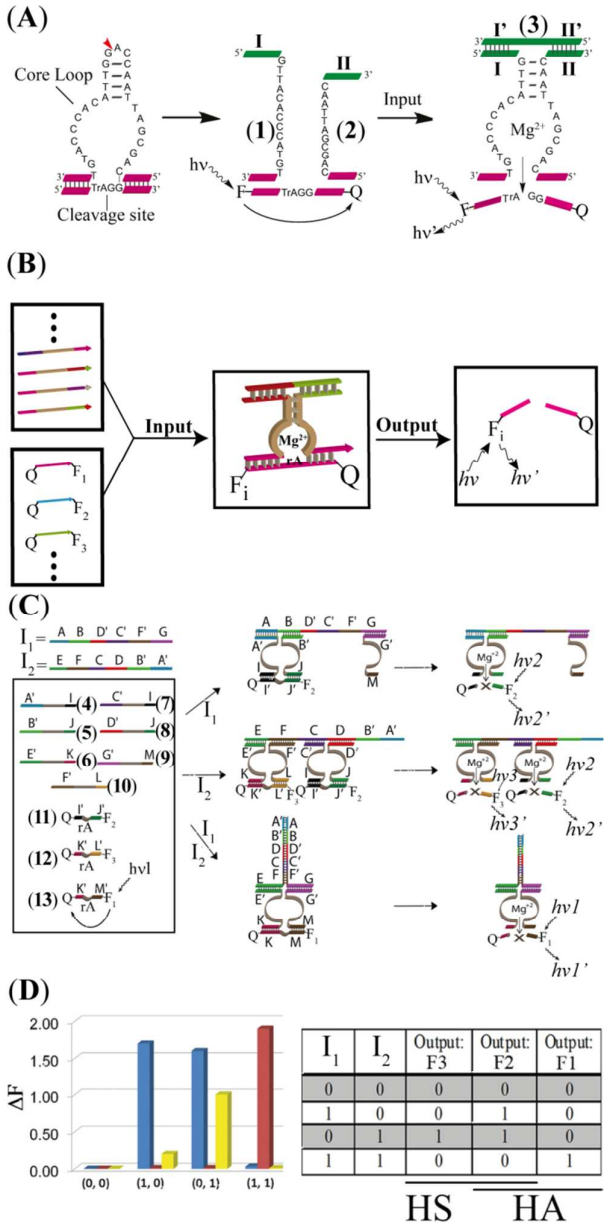

I_1	I_2	Output: F3	Output: F2	Output: F1
0	0	0	0	0
1	0	0	1	0
0	1	1	1	0
1	1	0	0	1

Figure 2: The implementation of a library of the Mg^{2+}-dependent DNAzyme subunits and their substrates for the operation of a universal set of logic gates: (A) Schematic cleavage of the Mg^{2+}-dependent DNAzyme sequence into two subunits, and their reassembly into an active DNAzyme structure by means of an auxiliary strand, acting as input. (B) Schematic presentation of the input-guided selection of DNAzyme subunits and their assembly into a computation module composed of the input/DNAzyme subunits/substrate. The cleavage of the substrate yields the fluorescence readout signal (output). (C) The operation of HA and HS by the inputs guided assemblies of different DNAzyme nanostructures acting as computational modules. The inputs I_1 and I_2 and the fluorescence of F_1, F_2 and F_3 provide the outputs of the different computational modules. (D) Fluorescence intensities generated by the HA and HS systems in the form of a bar presentation (left) and truth-table (right). (Figures (A), (C) and (D) reproduced with permission from ref 27. Copyright 2010 Nature Publishing Group; Figure (B) adapted with permission from Ref. 29.The Royal Society of Chemistry).

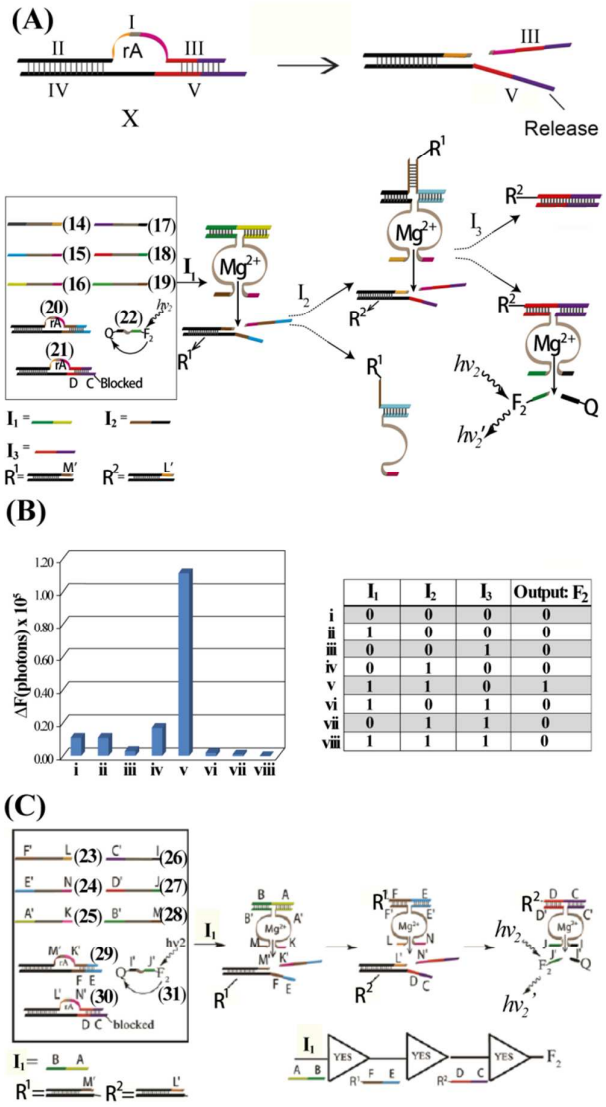

Figure 3: Operation of logic circuits using the Mg^{2+}-dependent DNAzyme subunits and substrates library and a series of inputs. (A) Schematic construct of the DNAzyme substrate that leads upon cleavage to a secondary input strand (top). Composition of the DNAzyme subunits/substrates and inputs leading to a sequence of computational modules that yield the YES-AND-InhibAND gate cascade via the cooperative generation of inputs through cleavage of the substrates. The fluorescence signal generated by the DNAzyme cascade provides the readout of the system (bottom). (B) Fluorescence intensities generated by the system subjected to the inputs I_2, I_2, I_3 following the states (i) – (viii) in the form of a bar presentation (left) and truth-table (right). The states (i) – (viii) are defined in the truth-table. (C) DNAzyme subunits/substrates and inputs leading to a sequence of computational modules that yield the YES-YES-YES cascade. (Reproduced with permission from ref 27. Copyright 2010 Nature Publishing Group).

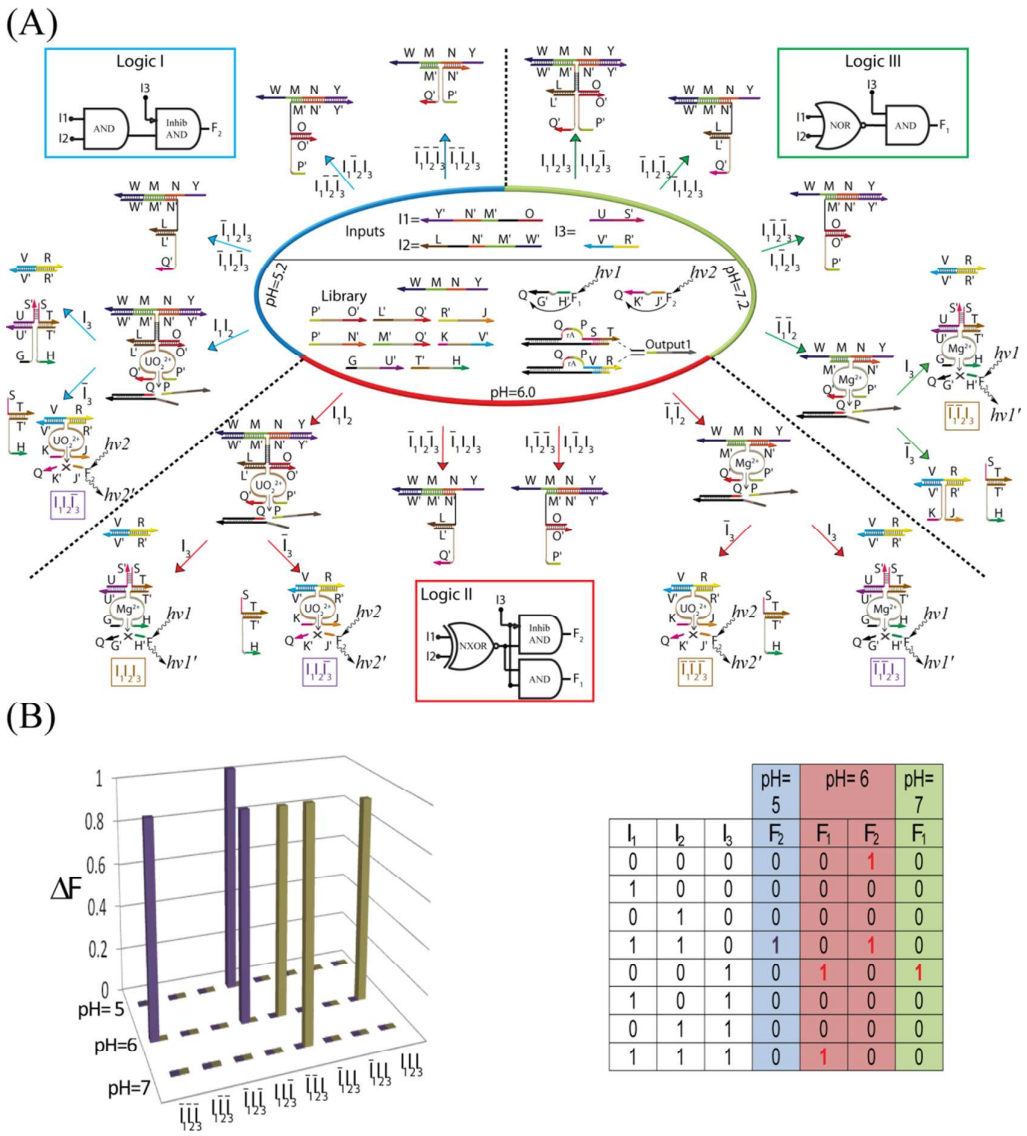

			pH= 5	pH= 6		pH= 7
I_1	I_2	I_3	F_2	F_1	F_2	F_1
0	0	0	0	0	1	0
1	0	0	0	0	0	0
0	1	0	0	0	0	0
1	1	0	1	0	1	0
0	0	1	0	1	0	1
1	0	1	0	0	0	0
0	1	1	0	0	0	0
1	1	1	0	1	0	0

Figure 4: pH-field programmable logic cascades using a library of two different pH-dependent DNAzymes subunits and their substrates. The DNAzymes include the Mg^{2+}-dependent DNAzyme (optimal activity at pH = 7.2) and the UO_2^{2+}-dependent DNAzyme (optimal activity at pH = 5.2). The two DNAzymes reveal partial activity at pH = 6.0. The substrates are labeled with the fluorophores F_1 and F_2 and their fluorescence reflect the operation of the computational modules of the Mg^{2+}-dependent DNAzyme and the UO_2^{2+}-dependent DNAzyme, respectively. The library subjected to I_1, I_2, I_3 yields at pH = 5.2 the logic I cascade, at pH = 6.0 the logic II cascade, and at pH = 7.2 the logic III cascade. (B) Fluorescence intensities of the different pH-programmed circuits in form of bar presentation (F_1- violet and F_2- brown) and the respective truth-table. (Reproduced with permission from ref 28. Copyright 2012 American Chemical Society).

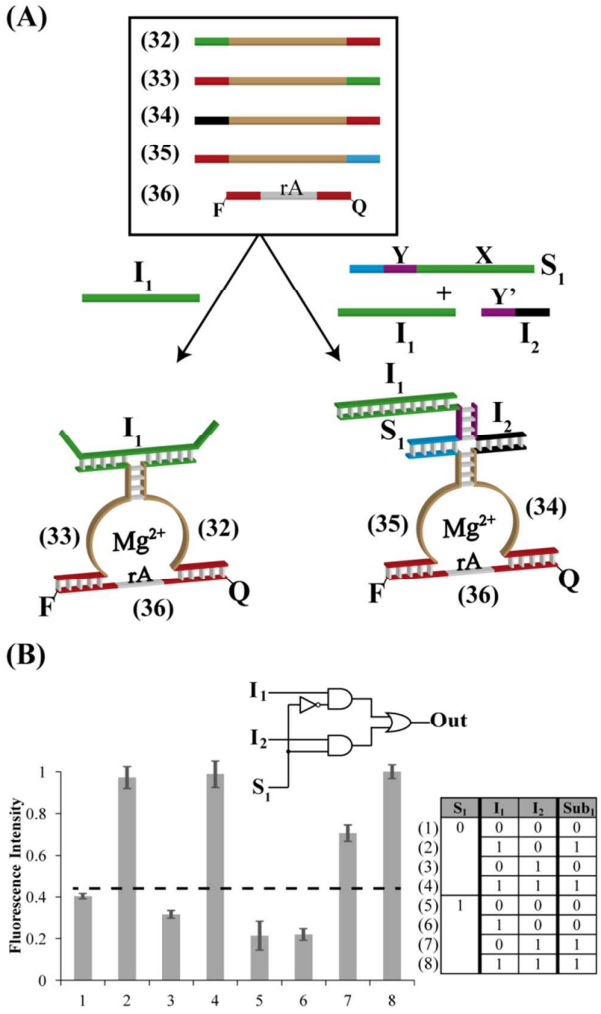

Figure 5: (A) Assembly of a 2:1 multiplexer, based on a library of the Mg^{2+}-dependent DNAzyme subunits and a fluorophore/quencher-functionalized substrate. (B) Fluorescence output intensities of the 2:1 multiplexer system subjected to the inputs I_1 and I_2 and the selector S_1 in the form of a bar presentation and accompanying truth-table. The different states of the inputs/selector are indicated in number (1) – (8). (Adapted with permission from Ref. 29.The Royal Society of Chemistry).

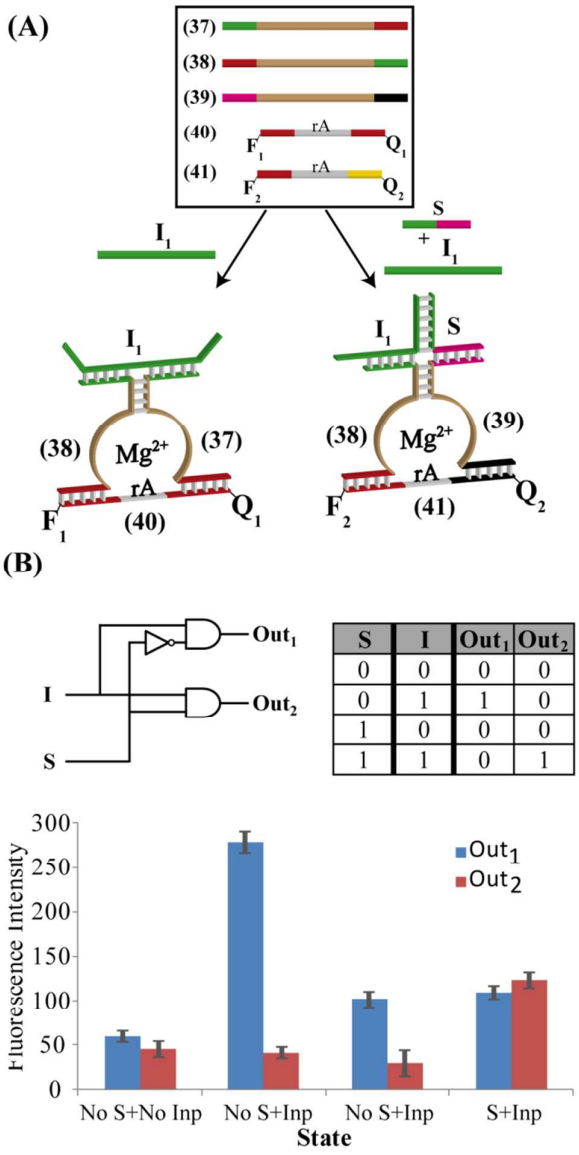

Figure 6: (A) Assembly of a 1:2 demultiplexer based on a library of the Mg^{2+}-dependent DNAzyme subunits and their fluorophore/quencher modified substrates. (Adapted from Ref. 29 with permission from The Royal Society of Chemistry). (B) Fluorescence intensities generated by the computing module in the presence of the input and selector in the form of fluorescence intensity bars and the respective truth-table. (Adapted with permission from Ref. 29.The Royal Society of Chemistry).

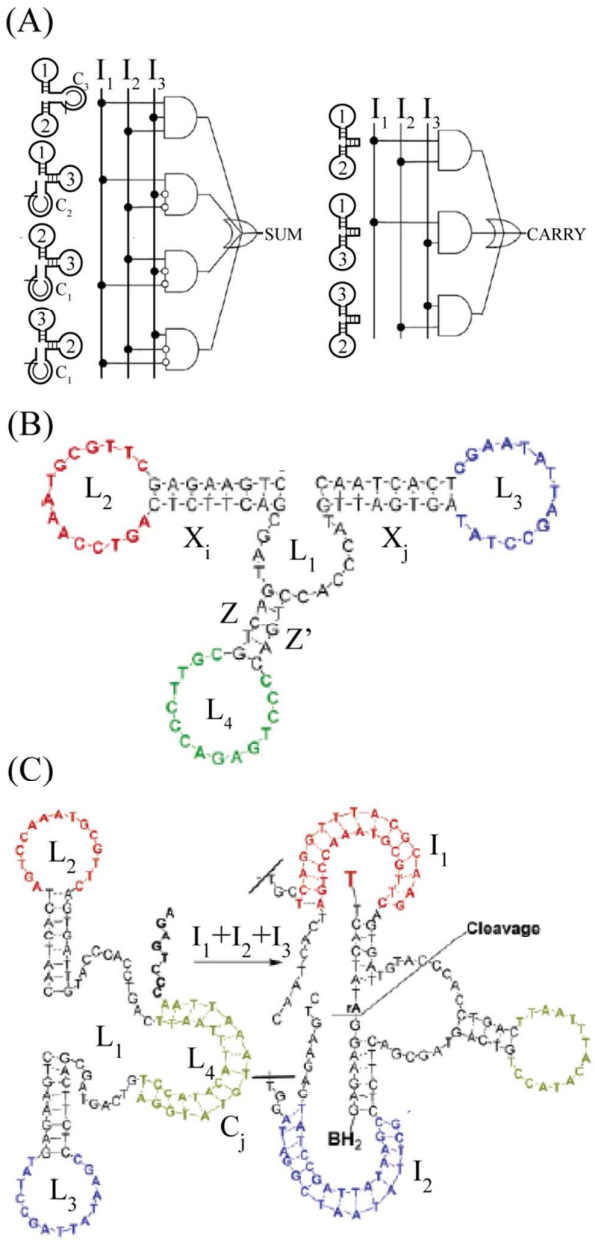

Figure 7: (A) Schematic illustration of the computing system. (B) DNA construct consisting of a "corona" of three hairpin units on a central nucleic acid loop that includes a DNAzyme sequence. The constructs provide the computational modules that lead to the fluorescence outputs. (C) Example of the interactions of the DNA construct with all three inputs. (Adapted with permission from ref 30. Copyright (2012) American Chemical Society).

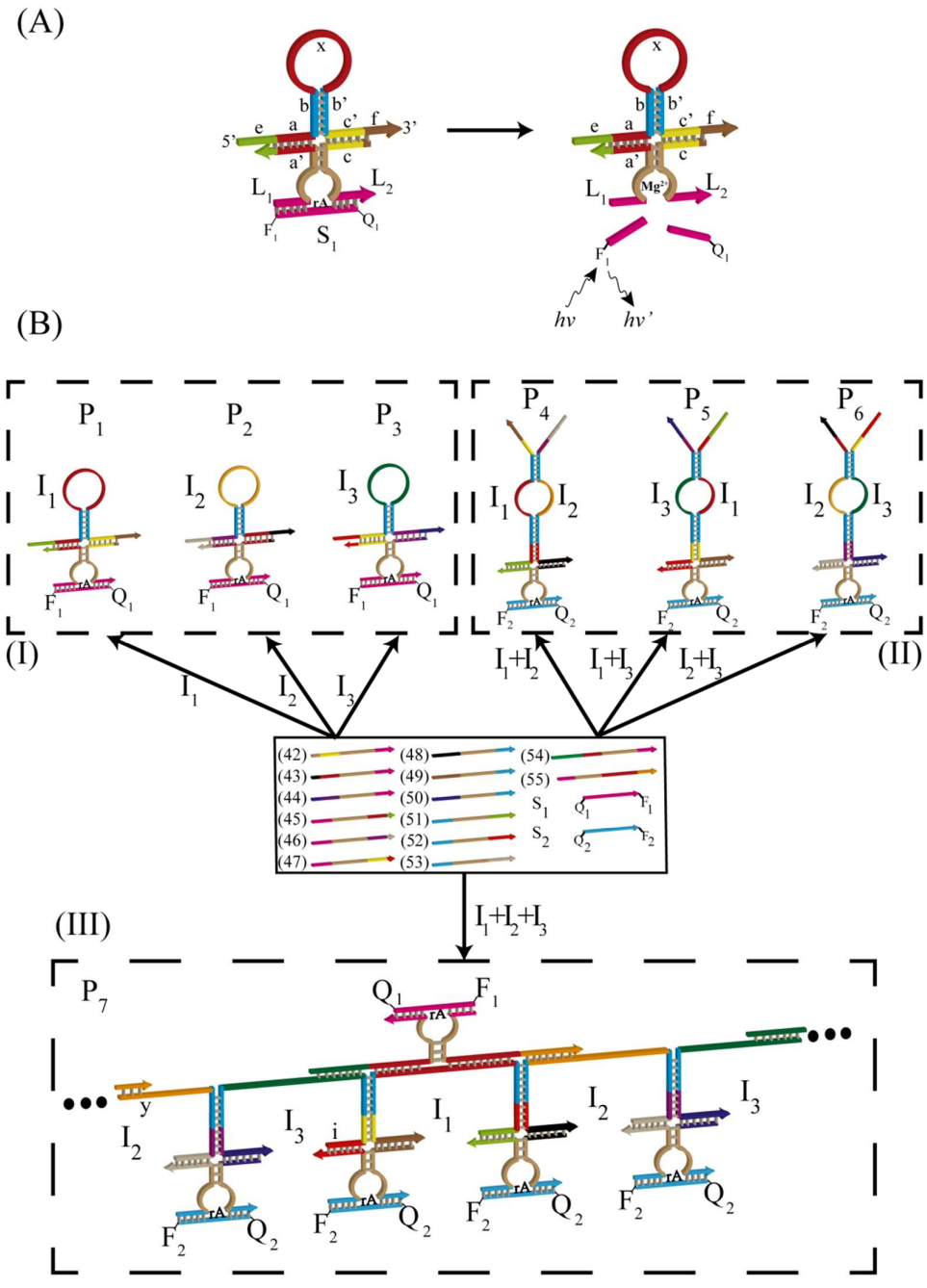

Figure 8: (A) Schematic construct of the library of the computational module for the Mg^{2+}-dependent DNAzyme-based full-adder. The inputs of the system include hairpin structures that guide the assembly of the respective Mg^{2+}-dependent DNAzymes. (B) Computing modules generated by the library of DNAzyme subunits and substrates upon operation of the full-adder in the presence of: Panel I – the individual inputs I_1, I_2 or I_3. Panel II – The combination of inputs $I_1 + I_2$; $I_1 + I_3$; $I_2 + I_3$. Panel III – In the presence of the mixture of all three inputs $I_1 + I_2 + I_3$. (Reproduced with permission from Ref. 31. The Royal Society of Chemistry).

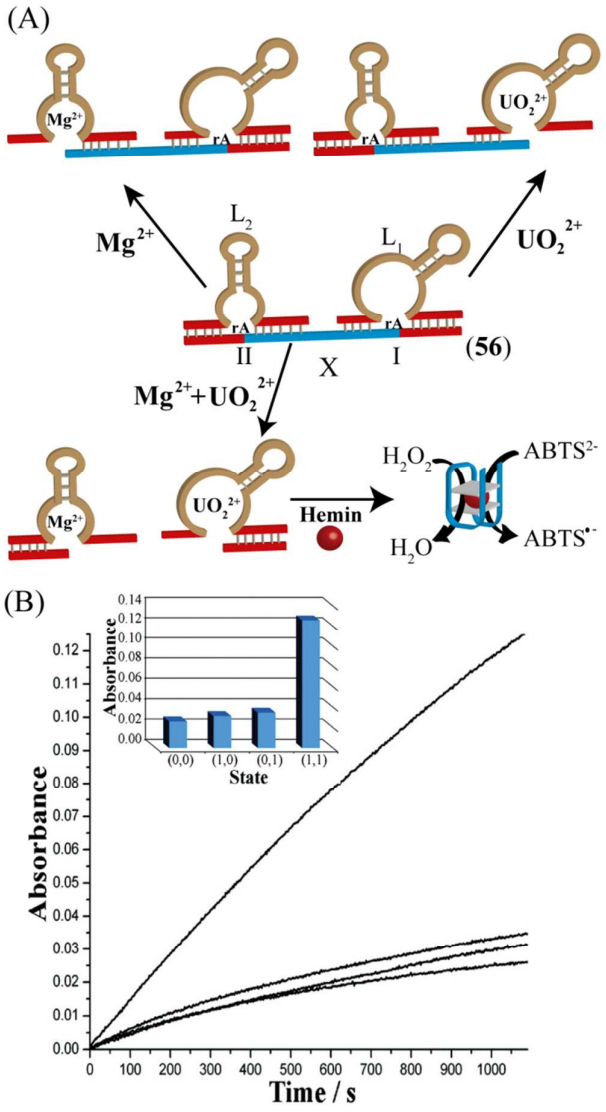

Figure 9: (A) Schematic operation of an AND gate consisting of the Mg^{2+}- and the UO_2^{2+}-dependent DNAzymes assembled on a DNA scaffold, composed of the substrates of the two DNAzymes that are separated by the G-quadruplex sequence. Only in the presence of the two inputs, Mg^{2+} and UO_2^{2+} ions, the scaffold is fragmented to form the hemin/G-quadruplex as catalytic trigger for the color output signal for the logic gate. (B) Time-dependent absorbance changes upon the operation of the logic AND gate. Absorbance changes originated from the hemin/G-quadruplex stimulated oxidation of $ABTS^{2-}$ to $ABTS^{\bullet-}$ by H_2O_2. Inset: Absorbance changes corresponding to the AND gate and presented in the form of absorbance intensity bars after a fixed time-interval of 18min. (Reproduced with permission from ref 32. Copyright (2009) American Chemical Society).

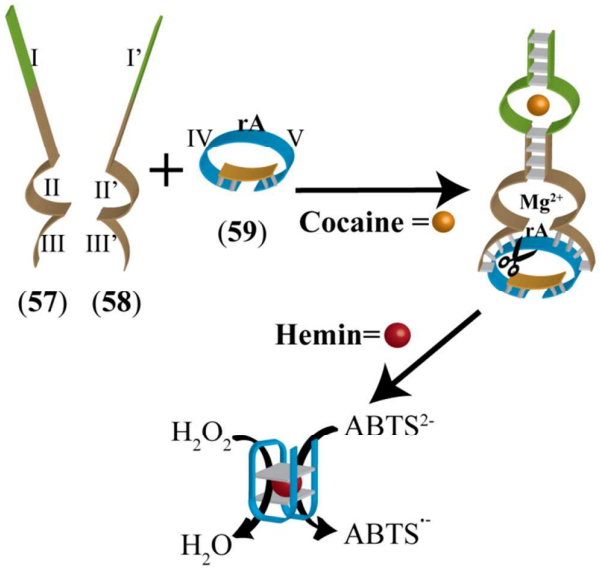

Figure 10: Schematic assembly of an AND logic gate through the input-guided assembly of the Mg^{2+}-dependent DNAzyme subunits, using Mg^{2+}-ions and cocaine as inputs. The cleavage of the quasi-circular substrate by the Mg^{2+}-dependent DNAzyme leads to the formation of the hemin/G-quadruplex DNAzyme that yields a colorimetric output signal.

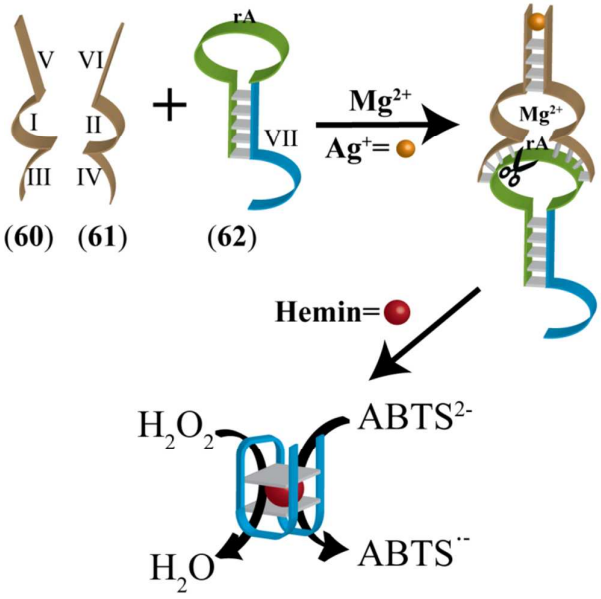

Figure 11: Assembly of an AND logic gate by the Ag^{+}-ion driven formation of the Mg^{2+}-dependent DNAzyme. Ag^{+} and Mg^{2+} act as inputs for the logic gate. The substrate (**62**) includes the G-quadruplex in a caged configuration. The input-driven assembly of the Mg^{2+}-dependent DNAzyme leads to the cleavage of the substrate and to the formation of the hemin/G-quadruplex as catalyst for the color output.

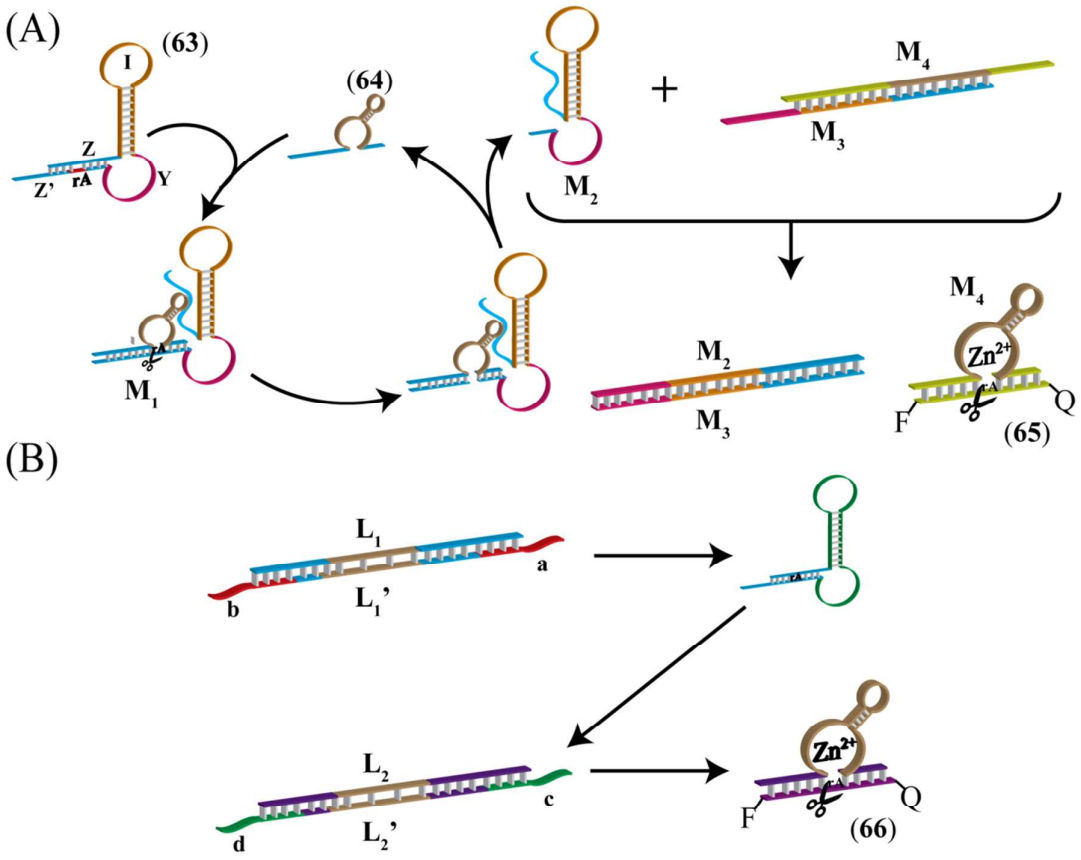

Figure 12: (A) A Multilayer Zn^{2+}-dependent DNAzyme cascade that includes a structured chimeric substrate, SCS, as functional scaffold. (B) Implementation of the multilayer Zn^{2+}-dependent DNAzyme cascade as a functional module for the sensing of conserved genome sequences of the dengue virus using the SCS as amplification scaffold for the synthesis of the Zn^{2+}-dependent DNAzymes participating in the sensing process.

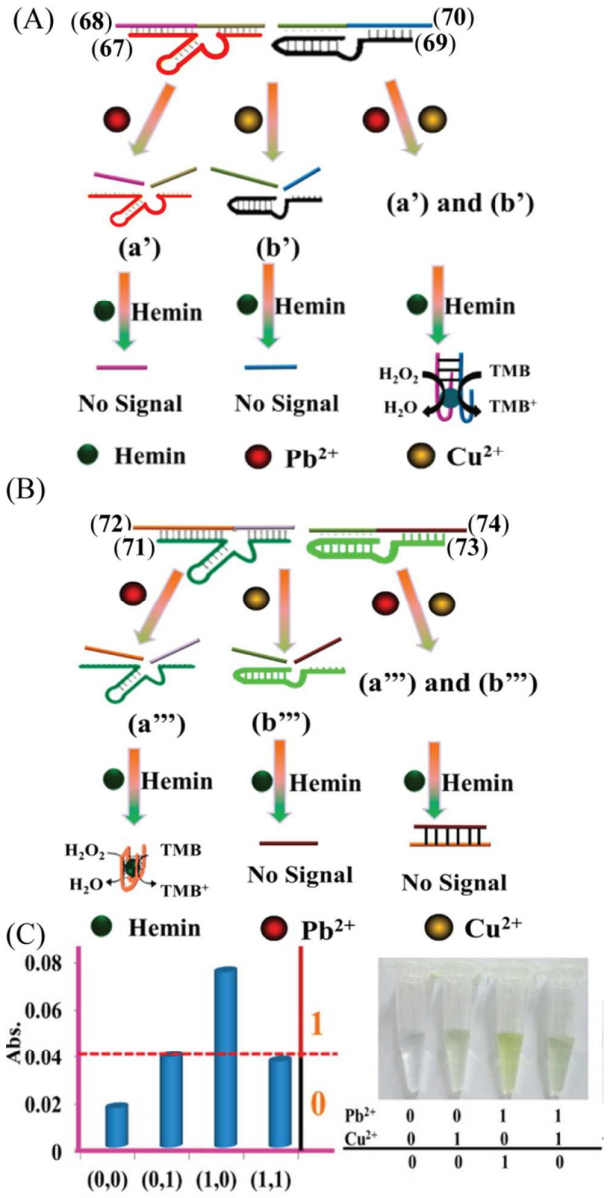

Figure 13: (A) Application of two different metal-dependent DNAzyme nanostructures for the operation of an AND gate using Pb^{2+} and Cu^{2+}-ions as inputs. (B) Design of two different metal-dependent DNAzyme nanostructures and their substrates, that operate as an INHIBIT gate. (C) Colorimetric output signals of the INHIBIT gate in the form of bars of absorbance intensities and visual monitoring of the gate operation. (Adapted with permission from ref 36. Copyright (2013) American Chemical Society).

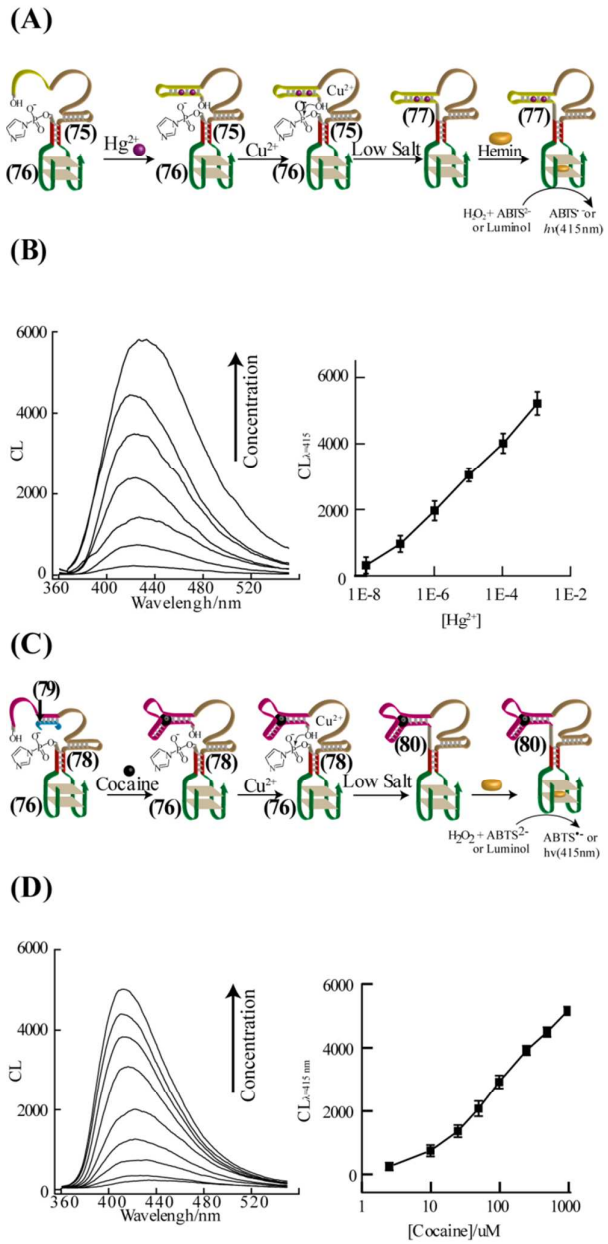

Figure 14: (A) Application of the Cu^{2+}-dependent ligation DNAzyme for the activation of an AND driven DNAzyme for sensing Hg^{2+}-ions, using Hg^{2+} and Cu^{2+} as inputs. (B) Chemiluminescence spectra generated by the AND gate driven DNAzyme cascade in the presence of different concentrations of Hg^{2+}-ions and the resulting calibration curve. (C) Application of the cocaine aptamer modified Cu^{2+}-dependent ligation DNAzyme as function unit for the AND gate driven operation of a DNAzyme cascade for sensing cocaine, using cocaine and Cu^{2+}-ions as inputs. (D) Chemiluminescence spectra generated by the AND gate driven DNAzyme cascade in the presence of variable concentrations of cocaine, and the derived calibration curve. (Reproduced with permission from ref 37. (Copyright 2012) Wiley-VCH).

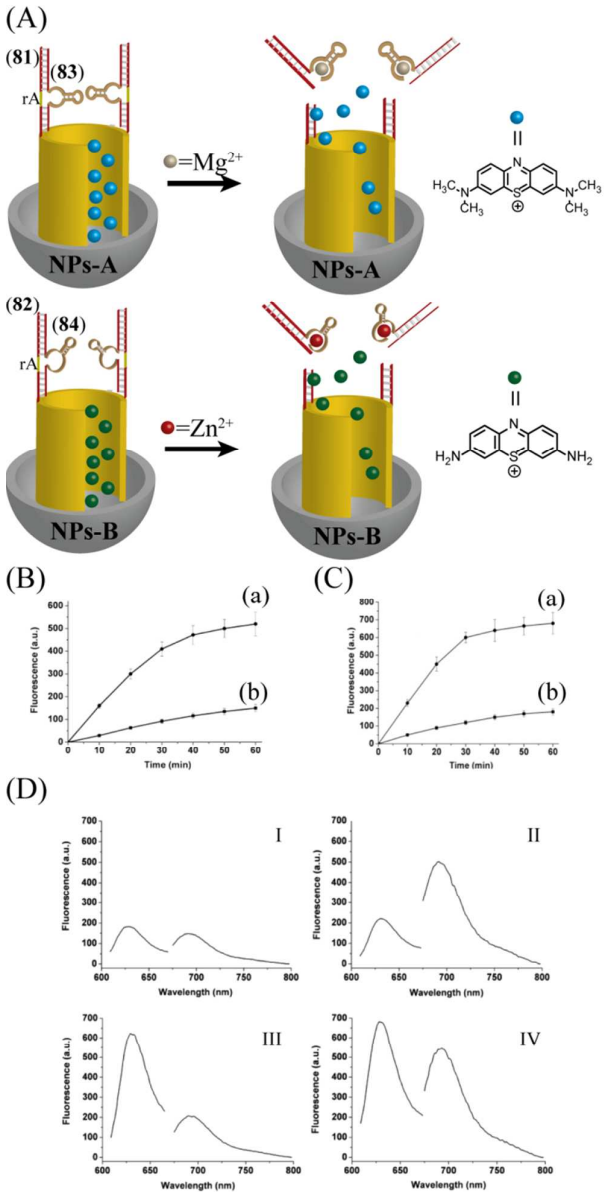

Figure 15: (A) Schematic AND logic gate release of two fluorescent dyes MB^+ and Th from DNAzyme-locked mesoporous SiO_2-NPs. The MB^+ dye is locked in pores capped by the Mg^{2+}-dependent DNAzyme sequence, (**74**)/(**72**). The Th dye is locked in the pores of mesoporous SiO_2-NPs capped by the Zn^{2+}-dependent DNAzyme sequence (**75**)/(**73**). The pores are unlocked in the presence of Mg^{2+} or Zn^{2+}-ions acting as inputs, the fluorescence of the released dyes provides output signals. (B) Time-dependent fluorescence changes of MB^+ upon: (a) Unlocking the pores with the Mg^{2+}-ions input. (b) In the absence of the Mg^{2+}-ion input. (C) Time-dependent fluorescence change of Th upon: (a) Unlocking the pores with the Zn^{2+}-ions input. (b) In the absence of Zn^{2+}. (D) Fluorescence spectra generated by the AND gate-driven release of MB^+ and Th from the capped mesoporous NPs subjected to: (I) No input (0, 0) (II) Only Mg^{2+}-ions (1, 0) (III) Only Zn^{2+}-ions (0, 1) (IV) Mg^{2+} and Zn^{2+}-ions (1, 1). (Reproduced with permission from ref 38. Copyright (2013) American Chemical Society).

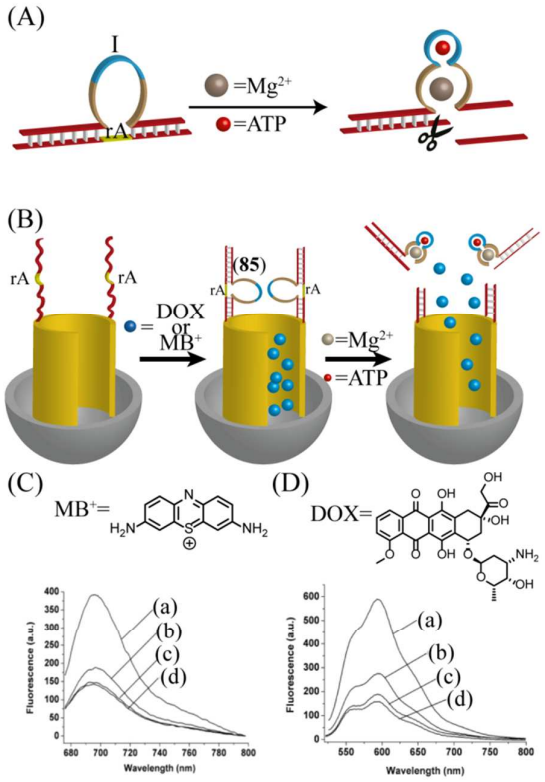

Figure 16: An AND logic gate unlocking mechanism of MB^+ or DOX, DOX-loaded mesoporous SiO_2 NPs using Mg^{2+} and ATP as inputs: (A) The design of the capping construct of a Mg^{2+}-dependent DNAzyme/substrate nanostructure being activated by the cooperative binding of Mg^{2+}-ions and ATP as inputs. (B) Schematic loading of MB^+ or DOX in the pores of the NPs using the DNAzyme/substrate construct as stimuli-responsive cap, and the unlocking of the pores in the presence of ATP and Mg^{2+} as triggering inputs (AND logic gate). (C) Selective release of MB^+ in the presence of ATP and Mg^{2+}, curve (a), release of MB^+ in the presence of Mg^{2+} or ATP, respectively, curves (b) and (c), release of MB^+ without any input, curve (d). (D) Selective release of DOX in the presence of ATP and Mg^{2+}, curve (a). Release of DOX in the presence of Mg^{2+} or ATP, respectively, curves (b) and (c). Release of DOX without any input, curve (d). (Reproduced with permission from ref 38. Copyright (2013) American Chemical Society).

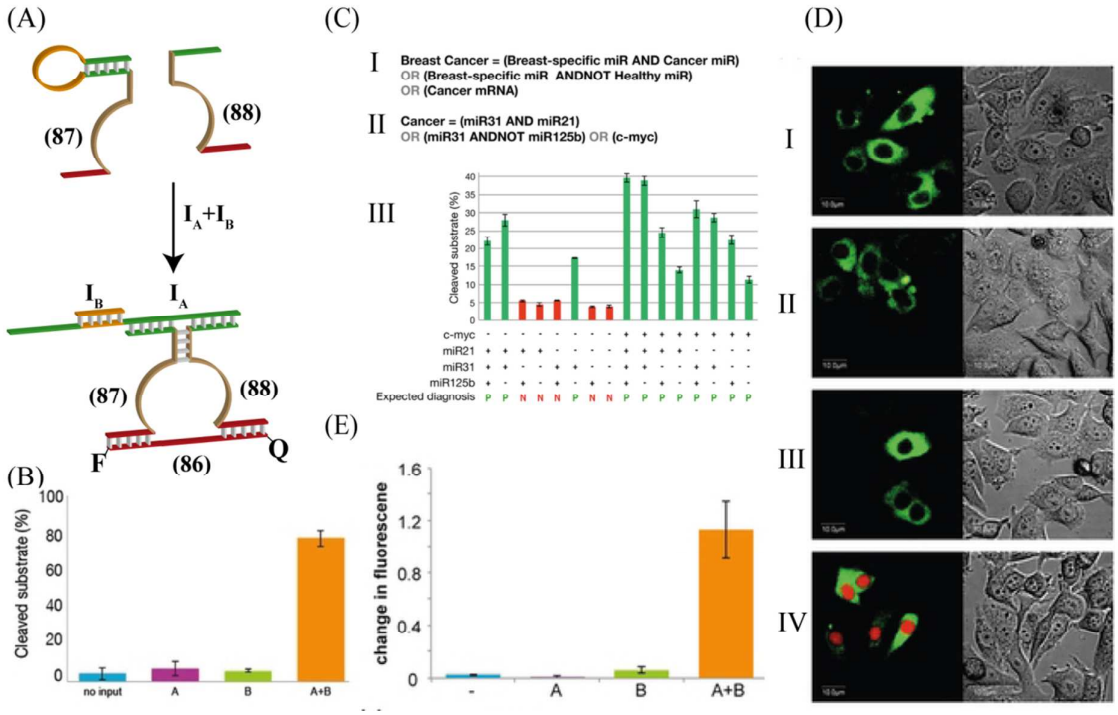

Figure 17: (A) Application of a library of c-jun cleaving Dz13 DNAzyme subunits and their substrates for the input-guides assembly of an AND gate computing module, where miR21 and miR125b act as inputs. Cleavage of the fluorophore/quencher-modified substrate leads to fluorescence as output signal. (B) Fluorescence intensities generated by the AND gate. (C) Fluorescence intensities generated in cell lysates by Boolean expression (Panel I or II) involving different input-guided combinations of computing modules that implement a variety of biomarkers. (D) Fluorescence and phase images of cells in which the AND gate subunits, its fluorescence/quencher modified substrate were incorporated and the cells were subjected to the respective miR-21 and miR-125b. Panel I – images with no input. Panel II – cell subjected to miR-21 only. Panel III – cells were subjected to miR-125b, only. Panel IV – cells were subjected to miR-21 and miR-125b. (E) Fluorescence intensities generated by the cells in the presence of the different inputs, confirming the miR-25 and miR-125b, stimulated AND gate operation. (Reproduced with permission from ref 39. Copyright (2013) Nature Publishing Group).

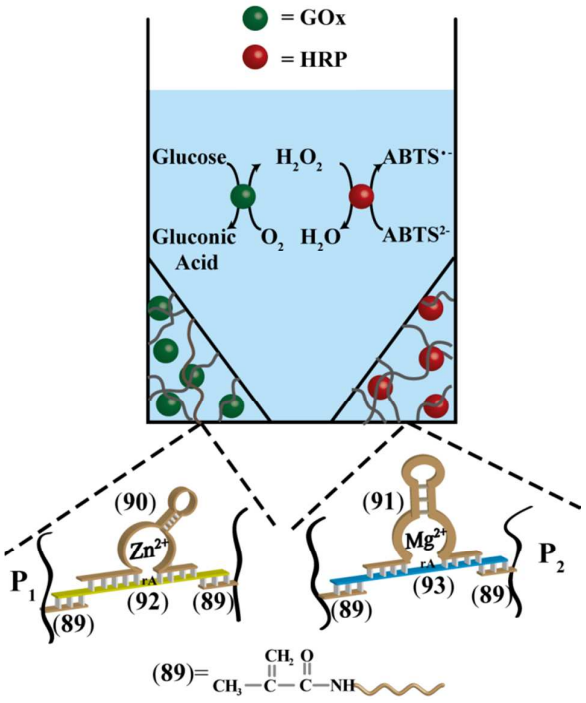

Figure 18: The AND logic gate driven release of GOx from the Zn^{2+}-dependent DNAzyme crosslinked hydrogel and of HRP from the Mg^{2+}-dependent DNAzyme crosslinked hydrogel, using Zn^{2+} and Mg^{2+} as inputs, and the activation of the bienzyme cascade.

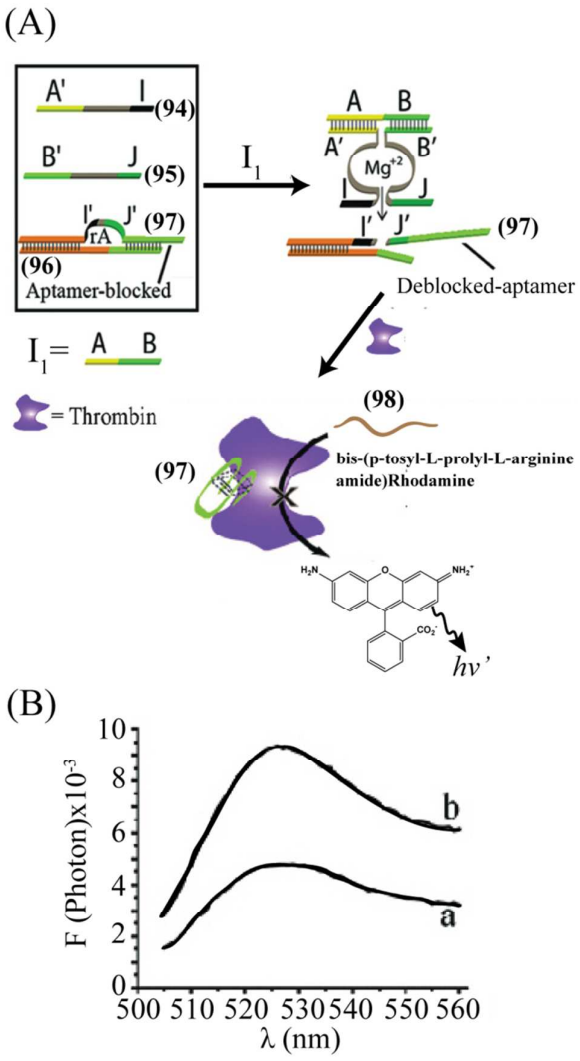

Figure 19: (A) The input-guided assembly of two subunits of the Mg^{2+}-dependent DNA that cleaves the substrate to yield the anti-thrombin aptamer sequence (**97**) as output. The released aptamer inhibits the thrombin-induced hydrolytic cleavage of the non-fluorescent Rhodamine-functionalized peptide (**98**). The cleavage of the peptide yield triggers-on the Rhodamine label. (B) Fluorescence spectra corresponding to: (a) The aptamer-inhibited cleavage of (**98**). (b) The non-inhibited cleavage of (**98**) in the presence of thrombin. (Adapted with permission from ref 27. Copyright 2010 Nature Publishing Group).